Trinity College Dublin
Coláiste na Tríonóide, Baile Átha Cliath
The University of Dublin

Coalgebra for Feynman Integrals

Eliza Somerville
Supervised by Professor Ruth Britto

Submitted in partial fulfilment of the
requirements for the degree of
B.A. Theoretical Physics

7 April 2024

Declaration

I have read and understood the plagiarism provisions in the General Regulations of the University Calendar for the current year, found at http://www.tcd.ie/calendar.

I have also read and understood the guide, and completed the 'Ready Steady Write' Tutorial on avoiding plagiarism, located at https://libguides.tcd.ie/academic-integrity/ready-steady-write.

Signed: Eliza Somerville

Date: 7 April 2024

Abstract

Feynman integrals are vital to precision calculations in quantum field theory, and are known to have a rich algebraic structure. In particular, the conjectured coaction principle postulates the existence of a mathematical operation called a coaction which enables Feynman integrals to be decomposed into pairs of simpler integrals. In recent years, one-loop Feynman integrals have been endowed with a diagrammatic coaction, which maps a given Feynman graph into pairs of graphs and cut graphs in a way that preserves the correspondence between graph and integral. We begin this report by providing an overview of the diagrammatic coaction at one loop, and discussing several simple examples. We then discuss other findings that support the coaction principle, based on the study of Feynman periods and the method of graphical functions. This method allows complicated Feynman graphs and their associated integrals to be built up recursively from simpler graphs. We conclude with a discussion of the potential for extending the diagrammatic coaction to multi-loop Feynman integrals. In particular, we perform a detailed study of the two-loop three-point ladder diagram, which has formed the main focus of our efforts in this project. This includes a reduction of the ladder diagram to a linear combination of master integrals, and the computation of several cuts of the ladder which are expected to appear in its diagrammatic coaction.

Acknowledgements

I'd like to thank my supervisor, Prof. Ruth Britto, for her excellent guidance throughout this project, and her very helpful advice during the preparation of this report. I'm also really grateful to my family and friends for their support.

Contents

1
Introduction

Feynman integrals are the key components involved in precision calculations in quantum field theory. In particular, they are crucial to the computation of scattering amplitudes, which enable predictions to be made about the results of high-energy collider experiments. However, the evaluation of Feynman integrals with multiple loops and multiple legs can be a major challenge. The search for more efficient methods of computing such integrals is likely to be aided by gaining a greater understanding of their algebraic structure.

In recent years, it has been conjectured that Feynman integrals obey a *coaction principle* [1], which postulates the existence of a mathematical operation called a *coaction* which allows Feynman integrals to be decomposed into linear combinations of pairs of integrals, where one member of each pair is itself a Feynman integral. There is a large body of evidence in support of this principle. In particular, it has been realised over the past two decades that a large number of Feynman integrals can be written in terms of multiple polylogarithms (MPLs). MPLs form a class of functions that generalise the ordinary logarithm and classical polylogarithms to several variables, and are endowed with a coaction. This realisation has led to the development of new techniques which have allowed Feynman integrals to be computed more efficiently.

However, for Feynman integrals with two or more loops, there are known to be cases which cannot be expressed in terms of MPLs alone. It is therefore desirable to generalise the coaction on MPLs to a coaction that acts on a larger class of functions. In recent years, a *diagrammatic coaction* has been constructed for one-loop Feynman integrals [2, 3], based on the graphical data of the associated Feynman diagram. This coaction involves the operations of *cutting* an edge, which corresponds to putting a propagator on mass-shell, and *pinching* an edge, which corresponds to eliminating a propagator and identifying the two vertices at its endpoints. In particular, the diagrammatic coaction maps a Feynman graph to a linear combination of pairs of graphs in which a subset of the internal edges have been cut or pinched. The cutting and pinching of the edges of the graph can be interpreted as operations being performed on the integral, so that the diagrammatic coaction has a one-to-one correspondence with a coaction on integrals. When acting on MPLs, the diagrammatic coaction reduces to the known coaction on these functions [3].

In addition to its ability to generalise the coaction beyond MPLs, a notable advantage of the diagrammatic approach is that diagrams impose physical consistency, which can help to constrain the set of possible terms in the coaction. The diagrammatic coaction on one-loop Feynman integrals with multiple legs is well understood [2, 3], but there are difficulties associated with extending it to diagrams with multiple loops. The first steps towards a generalisation to Feynman integrals with more than one loop were taken in [4].

Other evidence in support of the coaction principle has come from the study of *Feynman periods*, which are Feynman integrals which depend only trivially on external kinematics and thus evaluate to numbers, rather than functions. By including a minimal dependence on external kinematics, these periods can be generalised to *graphical functions*, which are massless three-point Feynman integrals parameterised to be functions on the complex plane. In [5], a set of transformation rules was defined on graphical functions and related conformal four-point integrals. When an operation is performed on

a Feynman graph, such as adding an edge or appending an external vertex, these transformation rules provide the corresponding analytic operation performed on the associated Feynman integral, allowing the correspondence between graph and integral to be preserved. This allows complicated Feynman graphs, and their corresponding integrals, to be built up by performing repeated transformations on a simple base graph, enabling the recursive computation of Feynman periods in arbitrary even dimensions. This method was used to compute a large number of Feynman periods in six-dimensional ϕ^3 theory up to seven loops in [5], and the results were observed to be compatible with the Feynman period version of the coaction conjecture.

In this report, we perform a study of the coalgebra structure of Feynman integrals, focusing particularly on the diagrammatic coaction. In Chapter 2, we review the diagrammatic coaction at one loop as set forward in [2], while in Chapter 3, we turn to the study of graphical functions and discuss their transformation rules as defined in [5], and we also discuss the family of generalised ladder graphs. In Chapter 4, we move on to discuss the potential extension of the diagrammatic coaction to two-loop Feynman graphs, focusing particularly on the two-loop three-point ladder diagram, which formed the central object of study in this project. This chapter includes the reduction of the ladder to a linear combination of master integrals, and the calculations of five of the relevant cut integrals. There is also a discussion of the difficulties associated with the computation of the sixth cut integral, and some potential methods for performing this calculation are suggested. Finally, in Chapter 5 we present our conclusions and discuss how this work could be extended in future.

In order to discuss the algebraic structure of Feynman integrals, we must first develop the necessary mathematical background. In the remainder of this chapter we introduce the class of functions known as multiple polylogarithms, which frequently arise in the computation of Feynman integrals. We then introduce the concepts of Hopf algebras and coactions, which will be essential for the discussion of the diagrammatic coaction in later chapters. We conclude the chapter by introducing one-loop Feynman integrals and cut Feynman integrals, and discussing some simple examples.

1.1 Multiple Polylogarithms

Multiple polylogarithms are a class of functions that generalise the classical polylogarithms to several variables. Our interest in them here stems from the fact that they arise in the computation of a large class of Feynman integrals, and moreover that they may be endowed with a coaction operation. In this section, we define the integral and sum representations of the multiple polylogarithms and discuss some of their properties, based on the treatment in [6, Chapter 8].

Integral Representation

We begin by defining the multiple polylogarithm $G(z_1, \ldots, z_n; y)$ for $y, z_i \in \mathbb{C}$ where all z_i are equal to zero by

$$G(\underbrace{0, \ldots, 0}_{n \text{ times}}; y) = \frac{1}{n!} \log^n(y). \tag{1.1}$$

If at least one z_i is nonzero, then we recursively define

$$G(z_1, z_2, \ldots, z_n; y) = \int_0^y \frac{dt}{t - z_1} G(z_2, \ldots, z_n; t). \tag{1.2}$$

We say that $G(z_1, \ldots, z_n; y)$ has a *trailing zero* if $z_n = 0$. For multiple polylogarithms without trailing zeros, the recursive definition gives

$$G(z_1, \ldots, z_n; y) = \int_0^y \frac{dt_1}{t_1 - z_1} \int_0^{t_1} \frac{dt_2}{t_2 - z_2} \cdots \int_0^{t_{n-1}} \frac{dt_n}{t_n - z_n}. \tag{1.3}$$

Here, n is called the *weight* of the integral representation.

To make it easier to relate the integral representation of the multiple polylogarithms to the sum representation introduced in the following section, we introduce the notation

$$G_{m_1\dots m_k}(z_1,\dots,z_k;y) = G(\underbrace{0,\dots,0}_{m_1-1},z_1,\dots,z_{k-1},\underbrace{0,\dots,0}_{m_k-1},z_k;y), \tag{1.4}$$

where z_j is assumed to be nonzero for $j = 1,\dots,k$.

Before completing the definition of the multiple polylogarithms by introducing their shuffle relations, we discuss an alternative representation of these functions as nested sums.

Sum Representation

The sum representation of the multiple polylogarithms is defined by

$$\mathrm{Li}_{m_1\dots m_k}(x_1,\dots,x_k) = \sum_{n_1>n_2>\dots>n_k>0} \frac{x_1^{n_1}}{n_1^{m_1}}\cdots\frac{x_k^{n_k}}{n_k^{m_k}}. \tag{1.5}$$

This is a nested sum, which can also be expressed as

$$\mathrm{Li}_{m_1\dots m_k}(x_1,\dots,x_k) = \sum_{n_1=1}^{\infty}\frac{x_1^{n_1}}{n_1^{m_1}}\sum_{n_2=1}^{n_1-1}\frac{x_2^{n_2}}{n_2^{m_2}}\cdots\sum_{n_k=1}^{n_{k-1}-1}\frac{x_k^{n_k}}{n_k^{m_k}}, \tag{1.6}$$

with the convention that

$$\sum_{n=a}^{b} f(n) = 0 \text{ for } b<a. \tag{1.7}$$

The sum converges for

$$|x_1x_2\dots x_j| \le 1 \text{ for all } j\in\{1,\dots,k\} \text{ and } (m_1,x_1)\neq(1,1). \tag{1.8}$$

We will always assume that the arguments x_j satisfy (1.8). The number k is called the *depth* of the sum representation, while the number $m_1+\dots+m_k$ is called the *weight* of the multiple polylogarithm.

The integral and sum representations of the multiple polylogarithms are related according to

$$\mathrm{Li}_{m_1\dots m_k}(x_1,\dots,x_k) = (-1)^k G_{m_1\dots m_k}\left(\frac{1}{x_1},\frac{1}{x_1x_2},\dots,\frac{1}{x_1x_2\dots x_k};1\right), \tag{1.9}$$

and

$$G_{m_1\dots m_k}(z_1,\dots,z_k;y) = (-1)^k\,\mathrm{Li}_{m_1\dots m_k}\left(\frac{y}{z_1},\frac{z_1}{z_2},\dots,\frac{z_{k-1}}{z_k}\right). \tag{1.10}$$

The ordinary logarithm and classical polylogarithms are included as special cases of multiple polylogarithms. The classical polylogarithms are defined by

$$\mathrm{Li}_m(x) = \sum_{n=1}^{\infty}\frac{x^n}{n^m} = -G_m\left(\frac{1}{x};1\right). \tag{1.11}$$

The values of the multiple polylogarithms at $x_1=\dots=x_k=1$ are called the *multiple zeta values*, and are denoted by

$$\zeta_{m_1\dots m_k} = \mathrm{Li}_{m_1\dots m_k}(1,1,\dots,1) = (-1)^k G_{m_1\dots m_k}(1,\dots,1;1). \tag{1.12}$$

1.2 Hopf Algebras and Coactions

Hopf algebras are structures which have applications in numerous areas of physics, including particle physics [6]. In this section, we give the definition of a Hopf algebra, and introduce the closely related notion of a *coaction*. This operation allows certain functions that arise in Feynman integrals, including multiple polylogarithms, to be decomposed into pairs of simpler functions [2].

Hopf Algebras

A *bialgebra* is a unital associative algebra H together with two maps

$$\begin{aligned} \Delta &: H \to H \otimes H, \\ \varepsilon &: H \to \mathbb{Q}, \end{aligned} \tag{1.13}$$

called the *coproduct* and *counit* respectively, which satisfy the following properties:

1. The coproduct is coassociative:

$$(\Delta \otimes \mathrm{id})\Delta = (\mathrm{id} \otimes \Delta)\Delta. \tag{1.14}$$

2. Δ and ε are algebra homomorphisms: for all $a, b \in H$,

$$\begin{aligned} \Delta(a \cdot b) &= \Delta(a) \cdot \Delta(b), \\ \varepsilon(a \cdot b) &= \varepsilon(a) \cdot \varepsilon(b). \end{aligned} \tag{1.15}$$

3. The counit and coproduct are related by

$$(\varepsilon \otimes \mathrm{id})\Delta = (\mathrm{id} \otimes \varepsilon)\Delta = \mathrm{id}. \tag{1.16}$$

A *Hopf algebra* is a bialgebra H together with an additional map $S : H \to H$, called the *antipode*, which satisfies

$$\begin{aligned} &m(\mathrm{id} \otimes S)\Delta = m(S \otimes \mathrm{id})\Delta = \varepsilon, \\ &S(a \cdot b) = S(a) \cdot S(b) \quad \forall\, a, b \in H, \end{aligned} \tag{1.17}$$

where m denotes multiplication in H.

A *comodule* over H is a $\mathbb{Q}$-vector space A together with a linear map

$$\widetilde{\Delta} : A \to A \otimes H, \tag{1.18}$$

called a *coaction*, that satisfies

$$\begin{aligned} &\Big(\mathrm{id} \otimes \widetilde{\Delta}\Big)\widetilde{\Delta} = \Big(\widetilde{\Delta} \otimes \mathrm{id}\Big)\widetilde{\Delta}, \\ &(\mathrm{id} \otimes \varepsilon)\widetilde{\Delta} = \mathrm{id}. \end{aligned} \tag{1.19}$$

The Coaction on Multiple Polylogarithms

We now discuss the relevance of Hopf algebras to the multiple polylogarithms, based on the discussion in [2].

Let $\mathcal{A}$ denote the $\mathbb{Q}$-vector space spanned by all multiple polylogarithms. This can be turned into an algebra using the fact that iterated integrals form a shuffle algebra, with a shuffle product given by

$$G(z_1, z_2, \ldots, z_k; y) \cdot G(z_{k+1}, \ldots, z_r; y) = \sum_{\text{shuffles } \sigma} G(z_{\sigma(1)}, z_{\sigma(2)} \ldots z_{\sigma(r)}; y), \tag{1.20}$$

where a permutation σ is said to be a *shuffle* of $(1, \ldots, k)$ and $(k+1, \ldots, r)$ if in

$$(\sigma(1), \sigma(2), \ldots, \sigma(r)) \tag{1.21}$$

the relative order of $1, 2, \ldots, k$ and of $k+1, \ldots, r$ is preserved. The shuffle product preserves the weight, meaning that the shuffle product of two multiple polylogarithms of weights n_1 and n_2 is a linear combination of multiple polylogarithms of weight $n_1 + n_2$.

Moreover, the quotient space $\mathcal{H} = \mathcal{A}/(i\pi\mathcal{A})$ is conjectured to form a Hopf algebra, and in particular can be equipped with a coassociative coproduct Δ_{MPL} which respects multiplication and the weight.

In practice, we are usually more interested in the full algebra $\mathcal{A}$, where we retain all factors of $i\pi$. We can reintroduce $i\pi$ by considering the trivial comodule $\mathcal{A} = \mathbb{Q}[i\pi] \otimes \mathcal{H}$, in which case the coproduct is lifted to a *coaction* $\Delta_{\mathrm{MPL}} : \mathcal{A} \to \mathcal{A} \otimes \mathcal{H}$, which satisfies

$$\Delta_{\mathrm{MPL}}(i\pi) = i\pi \otimes 1. \tag{1.22}$$

As a result, the rightmost coaction component is only defined modulo $i\pi$.

The operations of taking discontinuities and differentiation interact with the coaction according to

$$\Delta_{\mathrm{MPL}} \operatorname{Disc} = (\operatorname{Disc} \otimes \mathrm{id}), \tag{1.23}$$

$$\Delta_{\mathrm{MPL}} \frac{\partial}{\partial z} = \left(\mathrm{id} \otimes \frac{\partial}{\partial z}\right); \tag{1.24}$$

that is, the operation of taking discontinuities acts only on the leftmost component, while the operation of taking derivatives acts only on the rightmost component.

For our purposes, the results of applying the coaction Δ_{MPL} to the ordinary logarithm and the classical polylogarithms will be of most interest:

$$\Delta_{\mathrm{MPL}}(\log z) = 1 \otimes \log z + \log z \otimes 1, \tag{1.25a}$$

$$\Delta_{\mathrm{MPL}}(\mathrm{Li}_n(z)) = 1 \otimes \mathrm{Li}_n(z) + \sum_{k=0}^{n-1} \frac{1}{k!} \mathrm{Li}_{n-k}(z) \otimes \log^k(z). \tag{1.25b}$$

1.3 Feynman Integrals

In the notation of [2], the scalar one-loop n-point Feynman integrals are defined as

$$I_n^D\big(\{p_i \cdot p_j\}; \{m_i^2\}; \epsilon\big) = e^{\gamma_E \epsilon} \int \frac{d^D k}{i\pi^{D/2}} \prod_{j=1}^{n} \frac{1}{(k - q_j)^2 - m_j^2 + i0}, \tag{1.26}$$

where $\gamma_E = \Gamma'(1)$ is the Euler-Mascheroni constant, and where we work in dimensional regularisation in $D = d - 2\epsilon$ dimensions, where d is an even positive integer and ϵ is a formal variable. We denote the loop momentum by k, while the external momenta are labelled by p_i and satisfy the conservation of momentum, $\sum_{i=1}^{n} p_i = 0$. We define q_j to be a linear combination of the external momenta such that the momentum carried by the propagator labelled by j is $k - q_j$. Thus q_j can be obtained by imposing momentum conservation at each vertex of the diagram corresponding to the integral I_n^D:

$$q_j = \sum_{i=1}^{n} c_{ji} p_i, \quad c_{ji} \in \{-1, 0, 1\}. \tag{1.27}$$

We define the loop momentum k to be the momentum carried by the propagator labelled by 1, so that $q_1 = 0$.

In [2], a convenient basis for all one-loop integrals was chosen to be

$$\widetilde{J}_n\big(\{p_i \cdot p_j\}; \{m_i^2\}; \epsilon\big) = I_n^{D_n}\big(\{p_i \cdot p_j\}; \{m_i^2\}; \epsilon\big), \tag{1.28}$$

where

$$D_n = \begin{cases} n - 2\epsilon & \text{for } n \text{ even}, \\ n + 1 - 2\epsilon & \text{for } n \text{ odd}. \end{cases} \tag{1.29}$$

Here, we note that the existence of dimensional shift identities means that instead of choosing master integrals for a fixed dimension D, we may choose different basis integrals to be evaluated in different dimensions. The integrals $\widetilde{J}_n$ form a particularly convenient basis because they expected to be expressible in terms of multiple polylogarithms of uniform weight, up to an overall algebraic factor. This indicates that all one-loop Feynman integrals can be expressed in terms of multiple polylogarithms [2].

Examples of Feynman Integrals

To better illustrate the form of the basis integrals, we now discuss some simple examples of one-loop Feynman diagrams and their corresponding integrals. The diagrams shown here follow the convention that massive propagators are represented by bold lines, while massless propagators are represented by normal lines.

The simplest example of a Feynman integral is the tadpole integral. This is a one-point integral, so taking $n = 1$ in (1.29) we see that using our conventions this diagram should be evaulated in $D = 2 - 2\epsilon$ dimensions. The integral is given by

$$= \widetilde{J}_1(m^2) = e^{\gamma_E \epsilon} \int \frac{d^D k}{i\pi^{D/2}} \frac{1}{k^2 - m^2 + i0}. \tag{1.30}$$

The next simplest case is the bubble integral. This is a two-point integral, so as in the case of the tadpole we will evaluate it in $D = 2 - 2\epsilon$ dimensions. In the most general case where the two propagators have masses m_1^2 and m_2^2, the integral is given by

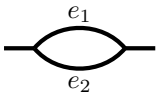

$$= \widetilde{J}_2(p^2; m_1^2, m_2^2) = e^{\gamma_E \epsilon} \int \frac{d^D k}{i\pi^{D/2}} \frac{1}{(k^2 - m_1^2 + i0)((k-p)^2 - m_2^2 + i0)}. \tag{1.31}$$

A third example which will be important in later chapters is that of the triangle diagram with three external scales and three massless propagators. This is a three-point integral, so we will evaluate it in $D = 4 - 2\epsilon$ dimensions. The integral is given by

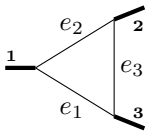

$$= \widetilde{J}_3(p_1^2, p_2^2, p_3^3) = e^{\gamma_E \epsilon} \int \frac{d^D k}{i\pi^{D/2}} \frac{1}{(k^2 + i0)((k-p_1)^2 + i0)((k-p_1-p_2)^2 + i0)}. \tag{1.32}$$

In this diagram, the number labelling each external edge indicates the index of the external momentum flowing through that edge.

1.4 Cut Feynman Integrals

We now introduce *cut Feynman integrals*, which play an important role in the diagrammatic coaction. A cut integral $\mathcal{C}_C \widetilde{J}_n$ is obtained by starting with a normal one-loop Feynman integral $\widetilde{J}_n$ and designating a subset C of propagators as *cut*. We call the remaining propagators *uncut*. Traditionally, the cut integral is computed by replacing the cut propagators by Dirac delta functions according to

$$\frac{1}{(k-q_j)^2 - m_j^2 + i0} \to -2\pi i \delta((k-q_j)^2 - m_j^2), \tag{1.33}$$

and then evaluating the integral under these constraints; this essentially corresponds to forcing the cut propagators on mass-shell.

It is important to note that cut Feynman integrals do not only appear in the formulation of the diagrammatic coaction. In fact, the concept of cut integrals originates from the cutting rules of Cutkosky [7]. The appearance of cut integrals in many different areas of study pertaining to the analytic structure of Feynman integrals stems from the fact that Feynman integrals are multi-valued functions, and cut integrals are related to the discontinuities of the original integral across its branch cuts [8]. In recent years, cut integrals have played a role in the study of integration-by-parts identities [9] and differential equations [10] satisfied by Feynman integrals.

However, the prescription (1.33) is not completely sufficient when studying the analytic structure of Feynman integrals, and a more precise definition of cuts is necessary. Such a definition was given for

one-loop cut integrals in [8], where they were defined as residues integrated over a well-defined contour in dimensional regularisation. To fully state this definition, we must introduce two determinants which can be applied to a subset of propagators $C \subseteq [n] = \{1, \ldots, n\}$. The first is the Gram determinant,

$$\mathrm{Gram}_C = \det((q_i - q_*) \cdot (q_j - q_*))_{i,j \in C \setminus *}, \tag{1.34}$$

where $*$ denotes any particular element of C. The second is the modified Cayley determinant,

$$Y_C = \det\left(\frac{1}{2}(-(q_i - q_j)^2 + m_i^2 + m_j^2)\right)_{i,j \in C}. \tag{1.35}$$

These can be used to classify the singularities of Feynman integrals into two types. A singularity of the first type corresponds to a kinematic configuration where Gram_C vanishes for a subset C of propagators. To such a singularity we associate a cut integral $\mathcal{C}_C \widetilde{J}_n$, where the integration contour is deformed so as to encircle the poles of the propagators in C. When this integral is evaluated in terms of residues, one obtains

$$\mathcal{C}_C \widetilde{J}_n = \frac{(2\pi i)^{\lfloor n_C/2 \rfloor} e^{\gamma_E \epsilon}}{(2i)^{n_C} \sqrt{Y_C}} \left(-\frac{Y_C}{\mathrm{Gram}_C}\right)^{(D_n - n_C)/2} \int \frac{d\Omega_{D_n - n_C}}{i\pi^{D_n/2}} \left[\prod_{j \neq C} \frac{1}{(k - q_j)^2 - m_j^2}\right]_C \mod i\pi, \tag{1.36}$$

where $n_C = |C|$ is the number of cut propagators, $[\cdot]_C$ indicates that the function inside the sqaure brackets is evaluated on the zero locus of the inverse cut propagators, and we assume Minkowski kinematics. Although this cut integral is only defined modulo $i\pi$, this will not impose a restriction on the computations relevant to the diagrammatic coaction because the second entry in the coaction is also defined modulo $i\pi$, as was discussed above.

A singularity of the second type corresponds to a configuration where Y_C vanishes for a subset C of propagators. To such a singularity we associate the cut integral $\mathcal{C}_{\infty C} \widetilde{J}_n$, where, as well as encircling the poles of propagators in C, the contour now also winds around the branch point at infinite loop momentum. It was shown in [8] that a cut integral associated to a singularity of the second type can be written as a linear combination of cut integrals associated to singularities of the first type as follows:

- For n_C even,

$$\mathcal{C}_{\infty C} \widetilde{J}_n = \sum_{i \in [n] \setminus C} \mathcal{C}_{C_i} \widetilde{J}_n + \sum_{\substack{i,j \in [n] \setminus C \\ i<j}} \mathcal{C}_{C_{ij}} \widetilde{J}_n \mod i\pi. \tag{1.37a}$$

- For n_C odd,

$$\mathcal{C}_{\infty C} \widetilde{J}_n = -2\mathcal{C}_C \widetilde{J}_n - \sum_{i \in [n] \setminus C} \mathcal{C}_{C_i} \widetilde{J}_n \mod i\pi. \tag{1.37b}$$

In the case where $C = \emptyset$, it can be shown that $\mathcal{C}_\infty \widetilde{J}_n = -\epsilon \widetilde{J}_n$ [2]. Combining this fact with the two relations above, we obtain the identity

$$\sum_{i \in [n]} \mathcal{C}_{C_i} \widetilde{J}_n + \sum_{\substack{i,j \in [n] \\ i<j}} \mathcal{C}_{C_{ij}} \widetilde{J}_n = -\epsilon \widetilde{J}_n \mod i\pi. \tag{1.38}$$

This provides a relation between the single and double cuts of an integral, and will play an important role in the cancellation of poles in the diagrammatic coaction.

The basis $\widetilde{J}_n$ of one-loop integrals can be lifted to a basis $\mathcal{C}_C \widetilde{J}_n$ of one-loop cut integrals, and (1.37a) and (1.37b) imply that the basis can be chosen to contain only cut integrals associated with singularities of the first type.

It is often convenient to normalise each basis integral $\widetilde{J}_n$ to its maximal cut in integer dimensions j_n, which is defined by

$$j_n \equiv \lim_{\epsilon\to 0} \mathcal{C}_{[n]} \widetilde{J}_n = \begin{cases} 2^{1-n/2} i^{n/2} Y_{[n]}^{-1/2}, & \text{for } n \text{ even}, \\ 2^{(1-n)/2} i^{(n-1)/2} \operatorname{Gram}_{[n]}^{-1/2}, & \text{for } n \text{ odd}. \end{cases} \tag{1.39}$$

Choosing this normalisation gives us the basis integrals

$$J_n = \widetilde{J}_n / j_n. \tag{1.40}$$

These are *pure* functions, meaning that the coefficients in their Laurent expansion in ϵ do not contain rational or algebraic functions of the external kinematic variables [11].

For future reference, we note that a one-loop cut integral with a single cut vanishes if the cut propagator is massless [8].

Examples of Maximal Cuts in Integer Dimensions

To illustrate some of the ideas just discussed, we will now compute the maximal cuts in integer dimensions of our three simple examples of Feynman integrals, by computing their maximal Gram determinants Gram_C or maximal modified Cayley determinants Y_C.

Tadpole Integral: In this simplest case, the maximal Gram determinant is

$$\operatorname{Gram}_{[1]} = 1, \tag{1.41}$$

so that according to (1.39), the maximal cut of the tadpole in two dimensions is simply

$$j_1 = \operatorname{Gram}_{[1]}^{-1/2} = 1. \tag{1.42}$$

Bubble Integral: For the bubble integral with two massive propagators, it is convenient to introduce two variables w and $\bar{w}$, defined such that

$$w\bar{w} = \frac{m_1^2}{p^2}, \quad (1-w)(1-\bar{w}) = \frac{m_2^2}{p^2}. \tag{1.43}$$

Then the maximal modified Cayley determinant can be expressed as

$$Y_{[2]} = \begin{vmatrix} m_1^2 & \frac{1}{2}(-p^2+m_1^2+m_2^2) \\ \frac{1}{2}(-p^2+m_1^2+m_2^2) & m_2^2 \end{vmatrix} = -\frac{1}{4}(p^2)^2(w-\bar{w})^2, \tag{1.44}$$

so that the maximal cut of the bubble in two dimensions is

$$j_2 = i Y_{[2]}^{-1/2} = -\frac{2}{p^2(w-\bar{w})}. \tag{1.45}$$

Triangle Integral: For the triangle integral with three external scales p_1^2, p_2^2, p_3^3 and three massless propagators, we introduce the variables z and $\bar{z}$ such that

$$z\bar{z} = \frac{p_2^2}{p_1^2}, \quad (1-z)(1-\bar{z}) = \frac{p_3^2}{p_1^2}. \tag{1.46}$$

In terms of these variables, the maximal Gram determinant is

$$\operatorname{Gram}_{[3]} = \begin{vmatrix} p_2^2 & p_2\cdot p_3 \\ p_2\cdot p_3 & p_3^2 \end{vmatrix} = p_2^2 p_3^2 - \frac{1}{4}(p_1^2-p_2^2-p_3^2)^2 = -\frac{1}{4}(p_1^2)^2(z-\bar{z})^2, \tag{1.47}$$

and the maximal cut of the triangle in four dimensions is

$$j_3 = \frac{i}{2}\operatorname{Gram}_{[3]}^{-1/2} = -\frac{1}{p_1^2(z-\bar{z})}. \tag{1.48}$$

2

The Diagrammatic Coaction at One Loop

The diagrammatic coaction is an operation that allows Feynman graphs to be decomposed into linear combinations of pairs of simpler graphs. It was first devised for one-loop graphs in [2, 3], and more recently steps have been taken to extend it to higher-loop graphs [4].

The utility of the diagrammatic coaction stems from the correspondence between Feynman graphs and Feynman integrals. In particular, the diagrammatic coaction has a one-to-one correspondence with a coaction on integrals. When acting on multiple polylogarithms, the diagrammatic coaction reduces to the known coaction on these functions [3].

In this chapter, we discuss the diagrammatic coaction at one loop, following the examples given in [2]. We will focus on the interpretation of Feynman integrals as Laurent expansions in the dimensional regulator ϵ, and the discussion will be centred on the *local coaction* which acts on the expansion coefficients. It should be noted that Feynman integrals can alternatively be interpreted as hypergeometric functions, and that there is a corresponding *global coaction* which acts on these functions [12]. However, we focus only on the local coaction in the following discussion.

2.1 The Diagrammatic Coaction

In order to discuss the diagrammatic coaction, we must first discuss the two main graphical operations that are involved. The first of these is the operations of *cutting* an edge, which has already been discussed briefly in the introduction, and corresponds to putting a propagator on mass-shell. The second operation is *pinching* an edge, which corresponds to eliminating a propagator and identifying the two vertices at its endpoints.

At one loop, the diagrammatic coaction is determined in terms of these operations by a simple rule first presented in [2], which may be stated as follows.

Rule for the Diagrammatic Coaction at One Loop

The second entries in the coaction run over cut integrals with the same propagators as the original integral, cutting all possible nonempty subsets of propagators. The form of each first entry depends on the parity of the number of cut edges in the corresponding second entry, and is determined as follows:

- if the number of cut edges is odd, then the first entry is the graph obtained by pinching the uncut edges;
- if the number of cut edges is even, then the first entry is the graph obtained by pinching the uncut edges, plus one-half times the sum of all graphs obtained by pinching an additional edge.

In the case of an odd number of cut propagators, the addition of one-half times the sum of all graphs obtained by pinching an additional edge may seem like an unjustified step. In fact, it is based on an understanding of the structure of singularities of one-loop Feynman integrals, and in particular is necessary to take into account the singularity at infinity [2].

2.2 Examples

In this section, we show that the rule given above for the diagrammatic coaction indeed reproduces the coaction on some simple examples of one-loop Feynman integrals, closely following the exposition in [2].

2.2.1 The Tadpole Integral

We begin with the simplest case of the tadpole integral in $D = 2 - 2\epsilon$ dimensions. This integral is given by

$$\widetilde{J}_1(m^2) = e^{\gamma_E \epsilon} \int \frac{d^D k}{i\pi^{D/2}} \frac{1}{k^2 - m^2 + i0} = -\frac{e^{\gamma_E \epsilon}\Gamma(1+\epsilon)(m^2)^{-\epsilon}}{\epsilon}, \tag{2.1}$$

while its only cut is given by

$$\mathcal{C}_e \widetilde{J}_1(m^2) = \frac{e^{\gamma_E \epsilon}\left(-m^2\right)^{-\epsilon}}{\Gamma(1-\epsilon)}. \tag{2.2}$$

Since $j_1 = 1$, these integrals are equivalent to their normalised forms J_1 and $\mathcal{C}_e J_1$. To compute the coaction on J_1, we use the fact that $\Delta(a \cdot b) = \Delta(a) \cdot \Delta(b)$, so that we can separately find the coaction on different factors in the expression. Firstly, to compute the coaction on $\left(m^2\right)^{-\epsilon}$, we expand this factor in ϵ as follows:

$$\left(m^2\right)^{-\epsilon} = e^{-\epsilon \log(m^2)} = \sum_{k=0}^{\infty} \frac{(-\epsilon)^k}{k} \log^k(m^2). \tag{2.3}$$

We can now use the linearity of the coaction and formula (1.25a) for the coaction on the ordinary logarithm to obtain [12]

$$\begin{aligned}\Delta_{\mathrm{MPL}}\left[\left(m^2\right)^{-\epsilon}\right] &= \sum_{k=0}^{\infty} \frac{(-\epsilon)^k}{k} \Delta_{\mathrm{MPL}}(\log^k(m^2)) = \sum_{k=0}^{\infty} \frac{(-\epsilon)^k}{k} \sum_{l=0}^{k} \binom{k}{l} \log^l(m^2) \otimes \log^{k-l}(m^2) \\ &= \sum_{k,l=0}^{\infty} \frac{(-\epsilon)^{k+l}}{k!l!} \log^l(m^2) \otimes \log^k(m^2) = \left(m^2\right)^{-\epsilon} \otimes \left(m^2\right)^{-\epsilon}. \end{aligned} \tag{2.4}$$

We note that this can be expressed as $\left(m^2\right)^{-\epsilon} \otimes \left(-m^2\right)^{-\epsilon}$, since the rightmost component of the coaction is only defined modulo $i\pi$, and

$$\left(-m^2\right)^{-\epsilon} = \left(m^2\right)^{-\epsilon}\left(1 - i\pi\epsilon + \frac{1}{2}(i\pi)^2\epsilon + \mathcal{O}(\epsilon^3)\right) = \left(m^2\right)^{-\epsilon} \mod i\pi. \tag{2.5}$$

We now turn to the factor $e^{\gamma_E \epsilon}\Gamma(1+\epsilon)$. We will make use of the identity

$$e^{\gamma_E \epsilon}\Gamma(1+\epsilon) = \exp\left(\sum_{k=2}^{\infty} \frac{(-\epsilon)^k}{k} \zeta_k\right) = \sum_{l=0}^{\infty} \frac{1}{l!}\left(\sum_{k=2}^{\infty} \frac{(-\epsilon)^k}{k} \zeta_k\right)^l, \tag{2.6}$$

which enables us to compute the coaction as follows:

$$\begin{aligned}\Delta_{\mathrm{MPL}}(e^{\gamma_E \epsilon}\Gamma(1+\epsilon)) &= \sum_{l=0}^{\infty} \frac{1}{l!}\left(\sum_{k=2}^{\infty} \frac{(-\epsilon)^k}{k} \Delta_{\mathrm{MPL}}(\zeta_k)\right)^l = \sum_{l=0}^{\infty} \frac{1}{l!}\left(\sum_{k=2}^{\infty} \frac{(-\epsilon)^k}{k} (\zeta_k \otimes 1 + 1 \otimes \zeta_k)\right)^l \\ &= \sum_{l=0}^{\infty} \frac{1}{l!} \sum_{m=0}^{l} \binom{l}{m} \left(\sum_{k=2}^{\infty} \frac{(-\epsilon)^k}{k} \zeta_k \otimes 1\right)^m \left(1 \otimes \sum_{j=2}^{\infty} \frac{(-\epsilon)^j}{j} \zeta_j\right)^{l-m} \\ &= \sum_{l,m=0}^{\infty} \frac{1}{l!m!} \left(\sum_{k=2}^{\infty} \frac{(-\epsilon)^k}{k} \zeta_k\right)^m \otimes \left(\sum_{j=2}^{\infty} \frac{(-\epsilon)^j}{j} \zeta_j\right)^l \\ &= e^{\gamma_E \epsilon}\Gamma(1+\epsilon) \otimes e^{\gamma_E \epsilon}\Gamma(1+\epsilon) = e^{\gamma_E \epsilon}\Gamma(1+\epsilon) \otimes \frac{e^{\gamma_E \epsilon}}{\Gamma(1-\epsilon)}, \end{aligned} \tag{2.7}$$

where in the final step, we have rewritten the rightmost component using the identity

$$\Gamma(1-\epsilon)\Gamma(1+\epsilon) = \frac{\pi\epsilon}{\sin(\pi\epsilon)} = 1 \mod i\pi. \tag{2.8}$$

We hence see that

$$\Delta_{\text{MPL}}\left[J_1\left(m^2\right)\right] = J_1\left(m^2\right) \otimes \mathcal{C}_e J_1\left(m^2\right), \tag{2.9}$$

or in graph form,

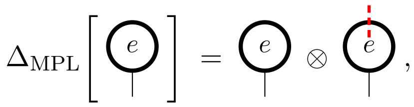

(2.10)

where the dashed red line represents a cut propagator. This agrees with the rule for the diagrammatic coaction stated in Section 2.1.

To check that this formula is consistent with the discontinuity criterion (1.23), we compute

$$\begin{aligned}
\text{disc}_{m^2}(m^2)^{-\epsilon} &= \frac{1}{2\pi i}\lim_{\eta\to 0}\left[(m^2+i\eta)^{-\epsilon} - (m^2-i\eta)^{-\epsilon}\right] \\
&= \frac{1}{2\pi i}\sum_{k=0}^{\infty}\frac{(-\epsilon)^k}{k!}\lim_{\eta\to 0}\left[\log^k(m^2+i\eta) - \log^k(m^2-i\eta)\right] \\
&= \theta(-m^2)\frac{1}{2\pi i}\sum_{k=0}^{\infty}\frac{(-\epsilon)^k}{k!}\left[\log^k(-m^2) - \left(\log(-m^2)+2\pi i\right)^k\right] \\
&= \theta(-m^2)\sum_{k=0}^{\infty}(-1)\frac{(-\epsilon)^k}{k!}k\log^{k-1}(-m^2) \mod i\pi \\
&= \theta(-m^2)\epsilon(-m^2)^{-\epsilon},
\end{aligned} \tag{2.11}$$

which gives

$$\text{disc}_{m^2} J_1(m^2) = \theta(-m^2)e^{\gamma_E\epsilon}\Gamma(1+\epsilon)(-m^2)^{-\epsilon} = \mathcal{C}_e J_1(m^2) \mod i\pi. \tag{2.12}$$

Taking the coaction, we obtain

$$\begin{aligned}
\Delta_{\text{MPL}}\left[\text{disc}_{m^2} J_1(m^2)\right] &= \theta(-m^2)\Delta_{\text{MPL}}\mathcal{C}_e J_1(m^2) \\
&= \theta(-m^2)\mathcal{C}_e J_1(m^2) \otimes \mathcal{C}_e J_1(m^2) \\
&= \left[\text{disc}_{m^2} J_1(m^2)\right] \otimes \mathcal{C}_e J_1(m^2),
\end{aligned} \tag{2.13}$$

which agrees with (1.23). One can similarly check that (2.10) is consistent with the differentiation property of the coaction, (1.24).

2.2.2 The Massless Bubble Integral

We now move on to discuss the bubble integral $\widetilde{J}_2(p^2)$ with two massless propagators in $D = 2-2\epsilon$ dimensions, which has the form

$$\widetilde{J}_2(p^2) = -\frac{2c_\Gamma}{\epsilon}\left(-p^2\right)^{-1-\epsilon}, \qquad c_\Gamma = \frac{e^{\gamma_E\epsilon}\Gamma^2(1-\epsilon)\Gamma(1+\epsilon)}{\Gamma(1-2\epsilon)}. \tag{2.14}$$

Since the propagators are massless, both single-propagator cuts of $\widetilde{J}_2(p^2)$ vanish. However the two-propagator cut is nonzero, and is given by

$$\mathcal{C}_{e_1e_2}\widetilde{J}_2(p^2) = -2\frac{e^{\gamma_E\epsilon}\Gamma(1-\epsilon)}{\Gamma(1-2\epsilon)}(p^2)^{-1-\epsilon}. \tag{2.15}$$

Normalising these expressions to the maximal cut j_2 given in (1.45) (where $w - \bar{w} = 1$ for the case of massless propagators), we obtain

$$J_2(p^2) = -\frac{c_\Gamma}{\epsilon}(-p^2)^{-\epsilon}, \quad \mathcal{C}_{e_1e_2}J_2(p^2) = \frac{e^{\gamma_E\epsilon}\Gamma(1-\epsilon)}{\Gamma(1-2\epsilon)}(p^2)^{-\epsilon}. \tag{2.16}$$

To compute the coaction on c_Γ, it is convenient to factorise the expression as follows:

$$c_\Gamma = \{\Gamma(1-\epsilon)\Gamma(1+\epsilon)\}\left\{\left(e^{-\gamma_E\epsilon}\Gamma(1-\epsilon)\right)\right\}\left\{\left(e^{-2\gamma_E\epsilon}\Gamma(1-2\epsilon)\right)^{-1}\right\}. \tag{2.17}$$

For the first factor, we can use (2.8) to obtain

$$\Delta_{\text{MPL}}[\Gamma(1-\epsilon)\Gamma(1+\epsilon)] = \Gamma(1-\epsilon)\Gamma(1+\epsilon)\otimes 1. \tag{2.18}$$

For the second and third factors, we again make use of identity (2.6), and follow a similar procedure to that used for the tadpole to obtain

$$\begin{aligned}\Delta_{\text{MPL}}\left[e^{-\gamma_E\epsilon}\Gamma(1-\epsilon)\right] &= \left(e^{-\gamma_E\epsilon}\Gamma(1-\epsilon)\right)\otimes\left(e^{-\gamma_E\epsilon}\Gamma(1-\epsilon)\right),\\ \Delta_{\text{MPL}}\left[\frac{1}{e^{-2\gamma_E\epsilon}\Gamma(1-2\epsilon)}\right] &= \frac{1}{e^{-2\gamma_E\epsilon}\Gamma(1-2\epsilon)}\otimes\frac{1}{e^{-2\gamma_E\epsilon}\Gamma(1-2\epsilon)}.\end{aligned} \tag{2.19}$$

This gives

$$\Delta_{\text{MPL}}[c_\Gamma] = c_\Gamma\otimes\frac{e^{\gamma_E\epsilon}\Gamma(1-\epsilon)}{\Gamma(1-2\epsilon)}, \tag{2.20}$$

so that

$$\Delta_{\text{MPL}}\left[J_2(p^2)\right] = J_2(p^2)\otimes\mathcal{C}_{e_1e_2}J_2(p^2). \tag{2.21}$$

In graph form, this is

$\Delta_{\text{MPL}}\Big[$ 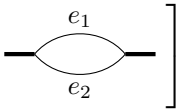 $\Big] =$ 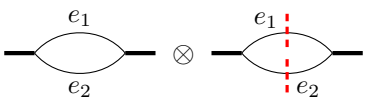 , (2.22)

which again agrees with the stated rule for the coaction.

2.2.3 The Triangle Integral with Three Massive Legs

The next example to be discussed is the triangle integral with massless internal propagators and three external masses p_i^2 for $i \in \{1,2,3\}$, in $D = 4-2\epsilon$. Focusing only on the leading term in the ϵ expansion, the integral and its normalised form are

$$\widetilde{J}_3(p_1^2,p_2^2,p_3^2) = \frac{(-p_1^2)^{-1-\epsilon}}{(z-\bar{z})}[\mathcal{T}(z,\bar{z})+\mathcal{O}(\epsilon)]; \quad J_3(p_1^2,p_2^2,p_3^2) = \mathcal{T}(z,\bar{z})+\mathcal{O}(\epsilon), \tag{2.23}$$

where the pure function $\mathcal{T}(z,\bar{z})$ is given by

$$\mathcal{T}(z,\bar{z}) = -2\,\text{Li}_2(z) + 2\,\text{Li}_2(\bar{z}) - \log(z\bar{z})\log\left(\frac{1-z}{1-\bar{z}}\right), \tag{2.24}$$

and its dimensionless arguments z and $\bar{z}$ are defined in (1.46). To compute the coaction on $\mathcal{T}(z,\bar{z})$, we use the result (1.25b) for the case $n = 2$,

$$\Delta_{\text{MPL}}[\text{Li}_2(z)] = 1\otimes\text{Li}_2(z) + \text{Li}_2(z)\otimes 1 - \log(1-z)\otimes\log z, \tag{2.25}$$

which gives

$$\begin{aligned}\Delta_{\text{MPL}}[\mathcal{T}(z,\bar{z})] &= \mathcal{T}(z,\bar{z})\otimes 1 + 1\otimes\mathcal{T}(z,\bar{z}) + \log(z\bar{z})\otimes\log\frac{1-\bar{z}}{1-z} \\ &\quad + \log[(1-z)(1-\bar{z})]\otimes\log\frac{z}{\bar{z}} \\ &= \mathcal{T}(z,\bar{z})\otimes 1 + 1\otimes\mathcal{T}(z,\bar{z}) + \log(-p_2^2)\otimes\log\frac{1-\bar{z}}{1-z} + \log(-p_3^2)\otimes\log\frac{z}{\bar{z}} \\ &\quad + \log(-p_1^2)\otimes\log\frac{\bar{z}(1-z)}{z(1-\bar{z})}. \end{aligned} \tag{2.26}$$

In the second line, we have rearranged terms to demonstrate that the formula satisfies the *first-entry condition*, which states that in the case of massless propagators, the terms in the coaction can be arranged so that all leftmost entries of weight one are logarithms of Mandelstam invariants [11].

We now want to show that this coaction can be written in terms of Feynman integrals and their cuts. We start with the term $\mathcal{T}(z,\bar{z})\otimes 1$, and use the results

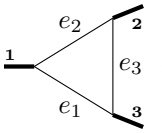

$= J_3 = \mathcal{T}(z,\bar{z}) + \mathcal{O}(\epsilon),$

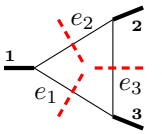

$= \mathcal{C}_{e_1e_2e_3} J_3 = 1 + \mathcal{O}(\epsilon).$ (2.27)

We thus see that the term $\mathcal{T}(z,\bar{z})\otimes 1$ can simply be expressed as

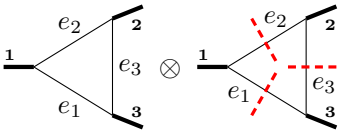

$= \mathcal{T}(z,\bar{z})\otimes 1 + \mathcal{O}(\epsilon).$ (2.28)

We now turn to the terms in the coaction in which both entries are of weight one,

$$\Delta_{1,1}[\mathcal{T}(z,\bar{z})] = \log(-p_1^2)\otimes\log\frac{\bar{z}(1-z)}{z(1-\bar{z})} + \log(-p_2^2)\otimes\log\frac{1-\bar{z}}{1-z} + \log(-p_3^2)\otimes\log\frac{z}{\bar{z}}. \tag{2.29}$$

Considering the results observed for the tadpole and bubble integrals, we expect that the logarithms in the second entries are related to the discontinuities of the triangle in one of the external scales; that is, we expect them to correspond to the two-propagator cuts of the triangle. Upon computing these cuts one obtains Gaussian hypergeometric functions [2], which to leading order yield

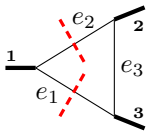

$= \mathcal{C}_{e_1e_2} J_3 = \log\frac{\bar{z}(1-z)}{z(1-\bar{z})} + \mathcal{O}(\epsilon),$

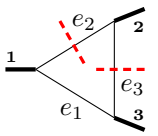

$= \mathcal{C}_{e_2e_3} J_3 = \log\frac{1-\bar{z}}{1-z} + \mathcal{O}(\epsilon),$ (2.30)

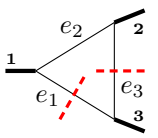

$= \mathcal{C}_{e_1e_3} J_3 = \log\frac{z}{\bar{z}} + \mathcal{O}(\epsilon).$

We also expect that each logarithm that forms one of the first entries of (2.29) can be expressed as a Feynman integral that has a discontinuity when the logarithms develop an imaginary part. One choice for such an integral is a bubble integral, which has the expansion

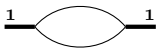

$$= J_2(p_1^2) = -\frac{1}{\epsilon} + \log(-p_1^2) + \mathcal{O}(\epsilon). \tag{2.31}$$

Focusing on the finite part of this integral, we see that (2.29) can be expressed as

$\Delta_{\text{MPL}}[\mathcal{T}(z,\bar{z})] =$

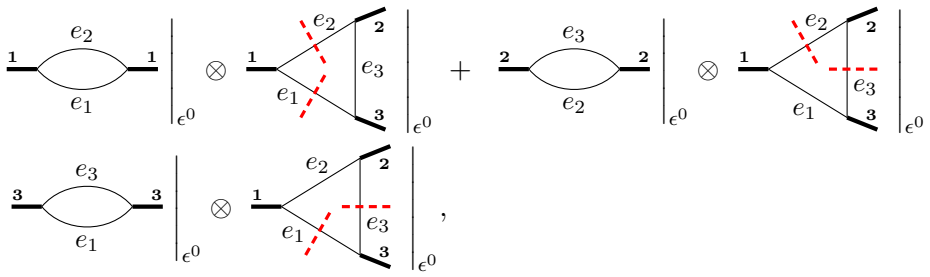

(2.32)

where $X|_{\epsilon^k}$ denotes the coefficient of ϵ^k in the Laurent expansion of X.

Finally, we must account for the poles of the bubble integrals and find an expression for the term $1 \otimes \mathcal{T}(z,\bar{z})$. We can achieve both of these aims using the identity (1.38) which relates a Feynman integral to a sum of its cuts, recalling that all single-propagator cuts of massless propagators vanish:

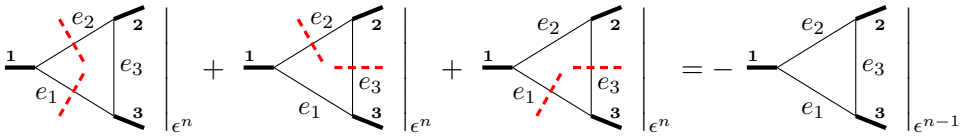

$$\text{mod } i\pi. \tag{2.33}$$

Setting $n = 1$ in this identity, we see that we can write

$1 \otimes \mathcal{T}(z,\bar{z}) =$

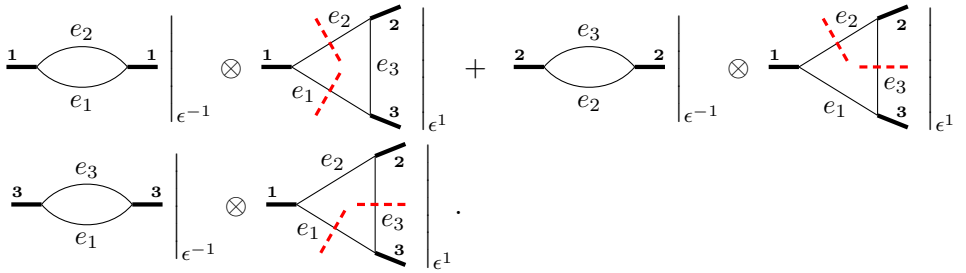

(2.34)

We also observe that this additional term cancels the poles introduced by the bubble integrals (2.31).

Combining all of these results, we see that up to $\mathcal{O}(\epsilon)$, we can write

$$\begin{aligned}\Delta_{\text{MPL}}\big[J_3(p_1^2,p_2^2,p_3^2)\big] &= J_2(p_1^2) \otimes \mathcal{C}_{e_1e_2} J_3(p_1^2,p_2^2,p_3^2) \\ &+ J_2(p_2^2) \otimes \mathcal{C}_{e_1e_2} J_3(p_1^2,p_2^2,p_3^2) + J_2(p_3^2) \otimes \mathcal{C}_{e_1e_2} J_3(p_1^2,p_2^2,p_3^2) \\ &+ J_3(p_1^2,p_2^2,p_3^2) \otimes \mathcal{C}_{e_1e_2e_3} J_3(p_1^2,p_2^2,p_3^2),\end{aligned}$$

which can be expressed in terms of graphs as

Δ_{MPL}

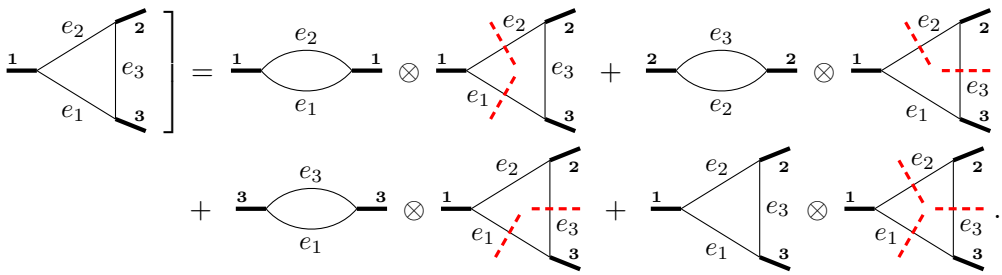

(2.35)

Again, this agrees with the stated rule for the diagrammatic coaction.

2.2.4 The Bubble Integral with Massive Propagators

In all three of the examples considered above, the graphical form of the coaction exhibits the same structure: the second entries run over cut integrals with the same propagators as the original integral, while the first entries are obtained from the original integral by pinching the uncut propagators of the corresponding right entry. However, this naive rule does not correctly reproduce the coaction on all one-loop Feynman integrals, as we will now see. This finding demonstrates the necessity of the additional pinched graphs included in the first entry when the number of cut edges is odd.

We consider the bubble integral whose propagators have masses m_1^2 and m_2^2. This integral is finite in $D = 2 - 2\epsilon$ dimensions, and to leading order is given by

$$\widetilde{J}_2(p^2; m_1^2, m_2^2) = \frac{1}{p^2(w-\bar{w})} \log\left(\frac{\bar{w}(1-w)}{w(1-\bar{w})}\right) + \mathcal{O}(\epsilon), \tag{2.36}$$

where the variables w and $\bar{w}$ are defined in (1.43). Normalising by j_2 given in (1.45) to obtain J_2, we see that the coaction on this function is

$$\Delta_{\text{MPL}}\left[J_2(p^2; m_1^2, m_2^2)\right] = \frac{1}{2}\left(\log\frac{w(1-\bar{w})}{\bar{w}(1-w)} \otimes 1 + 1 \otimes \log\frac{w(1-\bar{w})}{\bar{w}(1-w)}\right) + \mathcal{O}(\epsilon). \tag{2.37}$$

To analyse this coaction, we will need to use the ϵ-expansion of the massive tadpole diagram,

$$J_1(m_i^2) = \quad = -\frac{1}{\epsilon} + \log(m_i^2) + \mathcal{O}(\epsilon), \tag{2.38}$$

for $i = 1, 2$. We will also use the expansions of the normalised cuts of the massive bubble diagram (which are given to all orders in ϵ in terms of hypergeometric functions in [2]):

$$\mathcal{C}_{e_1} J_2 = \quad = -\frac{1}{2} + \mathcal{O}(\epsilon), \qquad \mathcal{C}_{e_2} J_2 = \quad = -\frac{1}{2} + \mathcal{O}(\epsilon),$$
$$\mathcal{C}_{e_1 e_2} J_2 = \quad = 1 + \mathcal{O}(\epsilon). \tag{2.39}$$

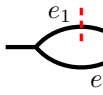

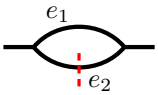

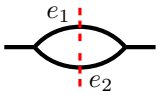

According to the naive rule which was observed to hold in the previous examples, the graphical form of the coaction (2.37) should be

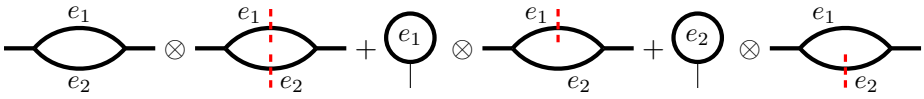

$$= \frac{1 \otimes 1}{\epsilon} + \mathcal{O}(\epsilon^0). \tag{2.40}$$

However, this expression has a pole in ϵ, whereas the expression in (2.37) clearly does not, so our simplistic expectation is not borne out in this case.

We claim, however, that the rule stated at the beginning of this chapter accurately reproduces the coaction on the bubble integral with massive propagators. We thus need to include additional terms in the first entries of the above formula, corresponding in each case to one-half times the sum of all graphs obtained by pinching an extra edge. Applying this rule, we obtain

$$\Delta_{\text{MPL}}\left[\quad\right] = \left(\quad + \frac{1}{2}\quad + \frac{1}{2}\quad\right) \otimes \quad$$
$$+ \quad \otimes \quad + \quad \otimes \quad . \tag{2.41}$$

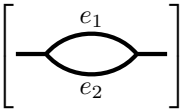

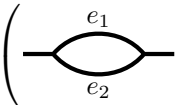

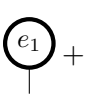

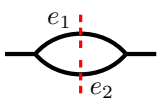

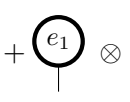

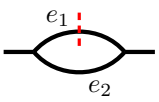

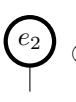

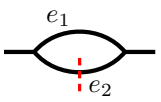

Examining this expression in light of (2.38) and (2.39), we see that the additional terms cause the pole in ϵ to cancel, and that we correctly reproduce the ϵ^0 term. We thus observe that the corrections made to the rule in the case of an odd number of cut propagators are indeed necessary to accurately reproduce the coaction in this case.

2.3 The Diagrammatic Coaction at Multiple Loops

As discussed in this chapter, the diagrammatic coaction at one loop is well-understood. The logical next step in the development of this field is the generalisation of the diagrammatic coaction to multi-loop integrals, and the first steps towards such a generalisation were taken in [4].

The analysis of the multi-loop case is substantially more challenging than that of the one-loop case for several reasons. One major difference in the multi-loop case is that there can be more than one master integral with the same set of propagators. Another is that there may be multiple independent contours that encircle the same set of poles, meaning that there may be several independent cuts which share the same set of on-shell propagators [4].

In Chapter 4, we will consider the example of the two-loop three-point ladder and attempt to find a diagrammatic representation of its coaction. This diagram is a member of the large class of ladder Feynman diagrams, and in the following chapter we discuss how such ladder diagrams may be constructed via the method of graphical functions.

3

Feynman Periods and Graphical Functions

In order to test any conjectured coaction formula, it is necessary to obtain data on a large number of Feynman integrals. Some of the simplest examples of such integrals are *Feynman periods*, which are Feynman integrals which depend only trivially on external kinematics. By including a minimal dependence on external kinematics, these periods can be generalised to *graphical functions*, which are massless three-point Feynman integrals parameterised to be functions on the complex plane.

One of the most attractive features of graphical functions is their adherence to a set of simple transformation rules. Many such rules were defined on graphical functions and related conformal four-point integrals in [5]. When an operation is performed on a Feynman graph, such as adding an edge or appending an external vertex, these transformation rules provide the corresponding analytic operation performed on the associated Feynman integral, allowing the correspondence between graph and integral to be preserved. This allows complicated Feynman graphs, and their corresponding integrals, to be built up by performing repeated transformations on a simple base graph, enabling the recursive computation of Feynman periods in arbitrary even dimensions. This provides an efficient method of collecting data to test a putative coaction defined on Feynman integrals. It was observed in [5] that the data obtained by this method for six-dimensional ϕ^3 theory supports the Feynman period version of the coaction conjecture.

In this chapter we introduce Feynman periods and graphical functions, and discuss some simple examples of their transformation properties. We also discuss the family of generalised ladder diagrams, and show how these are related to the momentum-space ladders via a conformal transformation.

3.1 Feynman Periods

Feynman periods are Feynman integrals which depend only trivially on external kinematics; equivalently, they are Feynman integrals of massless two-point functions. The computation of Feynman periods is a necessary part of many calculations in perturbative quantum field theory, such as the computation of renormalisation group functions in dimensional regularisation [13], and the evaluation of Feynman integrals in kinematic limits via the expansion by regions method [14].

Feynman periods are members of the wider class of numerical periods, which is a family of real numbers first defined by Kontsevich and Zagier [15]. They include all rational and algebraic numbers, but only certain transcendental numbers, including π, $\log 2$ and values of the Riemann ζ function evaluated at integer arguments [5].

3.2 Graphical Functions

Feynman periods can be generalised by allowing a minimal dependence on external kinematics, giving rise to the class of *graphical functions*. Graphical functions were first defined in [16], and the theory of their transformation rules was further developed in [17].

Graphical functions are obtained from specially parameterised Euclidean massless position-space Feynman integrals associated with graphs with three external vertices. Consider such a graph G with vertex set $\mathcal{V}_G$ and edge set $\mathcal{E}_G$. Let the set of external vertices be denoted by $\mathcal{V}_G^{\text{ext}}$, and the set of internal vertices by $\mathcal{V}_G^{\text{int}}$. The vertices are identified with vectors in D-dimensional Euclidean space; in particular, we label the external vertices by $\{x_a, x_b, x_c\} \subset \mathbb{R}^D$. Finally, let each edge $e \in \mathcal{E}_G$ have an associated weight ν_e. We then write the position-space three-point Feynman integral corresponding to the graph G as

$$I_G(x_a, x_b, x_c) = \int \left(\prod_{v \in \mathcal{V}_G^{\text{int}}} \frac{d^D y_v}{\pi^{D/2}} \prod_{e=\{v,w\} \in \mathcal{E}_G} \frac{1}{\|y_v - y_w\|^{(D-2)\nu_e}} \right), \tag{3.1}$$

where we integrate over $\mathbb{R}^D$ for each internal vertex. The integrand is the product of the massless position space propagators, where each propagator is a power of the Euclidean distance between the two incident vertices of the associated edge. If the incident vertex w is external, then the variable y_w is identified with the respective external variable x_a, x_b or x_c.

It is desirable to obtain an efficient parameterisation of the integral $I_G(x_a, x_b, x_c)$ which resolves its invariance under Poincaré invariance and scalings of x_a, x_b, x_c. This can be achieved by identifying the plane in $\mathbb{R}^D$ spanned by the vectors x_a, x_b, x_c with the complex plane $\mathbb{C}$, where we associate x_a with $0 \in \mathbb{C}$, x_b with $1 \in \mathbb{C}$, and x_c with a free parameter $z \in \mathbb{C}$. By identifying the standard metric on $\mathbb{C}$ with the Euclidean metric on $\mathbb{R}^D$ we obtain the identities

$$z\bar{z} = \frac{\|x_c - x_a\|^2}{\|x_a - x_b\|^2}, \qquad (1-z)(1-\bar{z}) = \frac{\|x_c - x_b\|^2}{\|x_a - x_b\|^2}. \tag{3.2}$$

The value of $I_G(x_a, x_b, x_c)$ can only depend on z, up to a trivial factor. We can therefore define a function $f_G : \mathbb{C} \to \mathbb{R}$ which captures the nontrivial dependence of I_G on the invariants,

$$f_G(z) = \frac{I_G(x_a, x_b, x_c)}{(\|x_a - x_b\|^2)^{-\omega_G}}, \tag{3.3}$$

where ω_G is the *position-space superficial degree of divergence* of G, defined by

$$\omega_G = \frac{D-2}{2} \sum_{e \in \mathcal{E}_G} \nu_e - \frac{D}{2} |\mathcal{V}_G^{\text{int}}|. \tag{3.4}$$

The function f_G is the *graphical function* associated with the graph G. For convenience, we usually label the external vertices x_a, x_b, x_c of G as $0, 1, z$ in correpsondence with the parameterisation chosen for the corresponding integral. The correspondence between the graph G and the function $f_G(z)$ can be represented as follows:

$G =$ 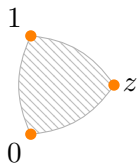

$\longleftrightarrow \qquad f_G(z),$ (3.5)

where we adopt the convention used in [5] whereby internal vertices are shown in black, external vertices are shown in orange, and the shaded region represents an arbitrary configuration of edges and internal vertices.

As mentioned above, a Feynman period is equivalent to a Euclidean position-space two-point Feynman integral, up to a scale factor. Such an integral corresponds to a graph G with two external vertices, and is the special case of (3.1) where there is no dependence on x_c. This implies that the

graphical function $f_G(z)$ defined in (3.3) is a constant; this constant is the position-space period P_G. Graphically, this correspondence can be represented as

$G =$ 

$\longleftrightarrow \qquad P_G = f_G(z).$ (3.6)

3.3 Transformation Rules for Graphical Functions

We now discuss some of the simplest transformation rules for graphical functions, closely following the presentation in [5]. Throughout this section, we use the definition $\lambda = D/2 - 1$; in the most familiar case of $D = 4$, this corresponds to $\lambda = 1$.

Adding edges between external vertices

Adding an edge of arbitrary weight between a pair of external vertices of a graph only changes the graphical function by a factor:

$G =$ 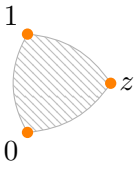

$f_G(z) = (z\bar{z})^{\lambda\nu_{0z}}((1-z)(1-\bar{z}))^{\lambda\nu_{1z}} f_{G'}(z)$

$\updownarrow \qquad\qquad \updownarrow$ (3.7)

$G' =$ 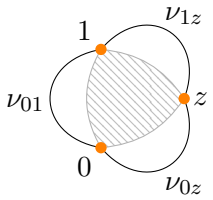

$f'_G(z) = (z\bar{z})^{-\lambda\nu_{0z}}((1-z)(1-\bar{z}))^{-\lambda\nu_{1z}} f_G(z).$

Note that adding an edge between the external vertices 0 and 1 leaves the graphical function unchanged.

Appending an external edge

The most important transformation rule involves appending an edge of weight 1 to the external vertex z while creating a new internal vertex. This enables complicated graphs, and their corresponding graphical functions, to be built up recursively from simpler cases. The associated transformation of the graphical function is

$G =$ 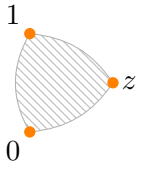

$f_G(z) = -\Gamma(\lambda)\dfrac{1}{(z-\bar{z})^\lambda}\Delta_{\lambda-1}(z-\bar{z})^\lambda f_{G'}(z)$

$\updownarrow \qquad\qquad \updownarrow$ (3.8)

$G' =$ 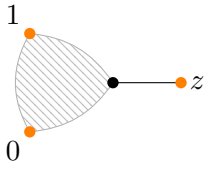

$f'_G(z) = -\dfrac{1}{\Gamma(\lambda)}\dfrac{1}{(z-\bar{z})^\lambda}\mathcal{I}_{\lambda-1}(z-\bar{z})^\lambda f_G(z),$

where $\Delta_{\lambda-1}$ is the effective Laplacian on graphical functions,

$$\Delta_{\lambda-1} = \partial_z \partial_{\bar{z}} + \frac{\lambda(\lambda-1)}{(z-\bar{z})^2}, \tag{3.9}$$

and $\mathcal{I}_{\lambda-1}$ is the integration operator that inverts the Laplacian, given by

$$\mathcal{I}_{\lambda-1} = \sum_{k,l=0}^{\lambda-1} c_{\lambda-1,k,l} \frac{1}{(z-\bar{z})^k} \int_{\mathrm{sv}} dz (z-\bar{z})^{k+l} \int_{\mathrm{sv}} d\bar{z} \frac{1}{(z-\bar{z})^l}, \tag{3.10}$$

where the coefficients are defined by $c_{n,k,l} = (-1)^{n+k+l} \frac{(n+k)!(n+l)!}{(n-k)!(n-l)!(k+l)!k!l!}$, and the single-valued integration operators $\int_{\mathrm{sv}} dz$ must be interpreted properly in a suitable function space, as discussed in [17].

Internalising a vertex

A graphical function can be transformed into a Feynman period by integrating over the external vertex z to make it internal. The corresponding transformation rule is

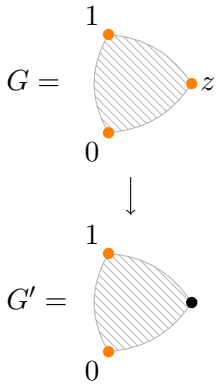

$$f_G(z) \qquad\qquad f'_G(z) = \frac{\Gamma(\lambda)}{\Gamma(2\lambda)} \int_{\mathbb{C}} \frac{dz\, d\bar{z}}{2\pi} \left(\frac{z-\bar{z}}{i}\right)^{2\lambda} f_G(z). \tag{3.11}$$

Completion of graphical functions

It is now convenient to introduce a slightly modified graphical representation, known as the *completion* of a Feynman graph. Completed graphical functions are conformal four-point integrals, and completion makes manifest the conformal invariance of the underlying massless Feynman integral.

To complete a graph G, we perform the following steps:

1. Add a new external vertex ∞ to the graph,
2. Add an edge from ∞ to each internal vertex, with a weight such that the total sum of the incident edge weights at the internal vertex is $2D/(D-2)$,
3. Add an edge between ∞ and the external vertex z with a weight such that the incident edge weight sum at z is zero,
4. Add edges between the three external vertices 0, 1 and ∞ such that the incident edge weight sum at each external vertex is zero.

This procedure produces a unique completed graph $\overline{G}$:

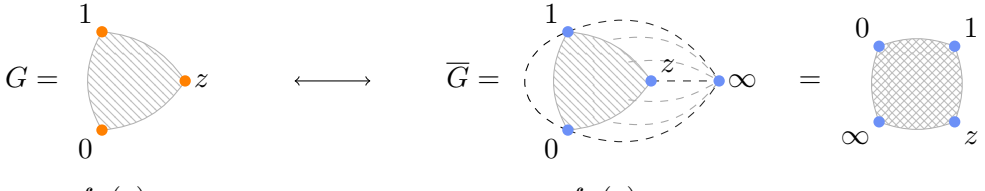

$$f_G(z) \qquad = \qquad f_{\overline{G}}(z). \tag{3.12}$$

Again adhering to the conventions of [5], we distinguish between completed and uncompleted graphs by colouring the external vertices blue in the completed case. It should be emphasised that completion is not a transformation of the graph, but merely a change in the graphical representation of the corresponding function [17].

Permutation of external vertices

A conformal four-point integral depends only on the cross-ratio of the four external positions. This means that the corresponding graphical function is invariant under double transpositions of the four external vertices.

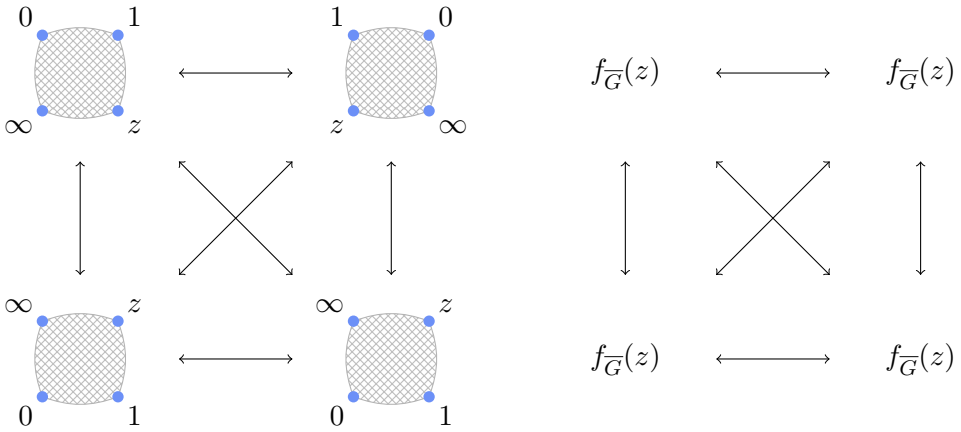

(3.13)

Permutations of the external vertices which are not double transpositions correpsond to Möbius transformations of the argument of the graphical function.

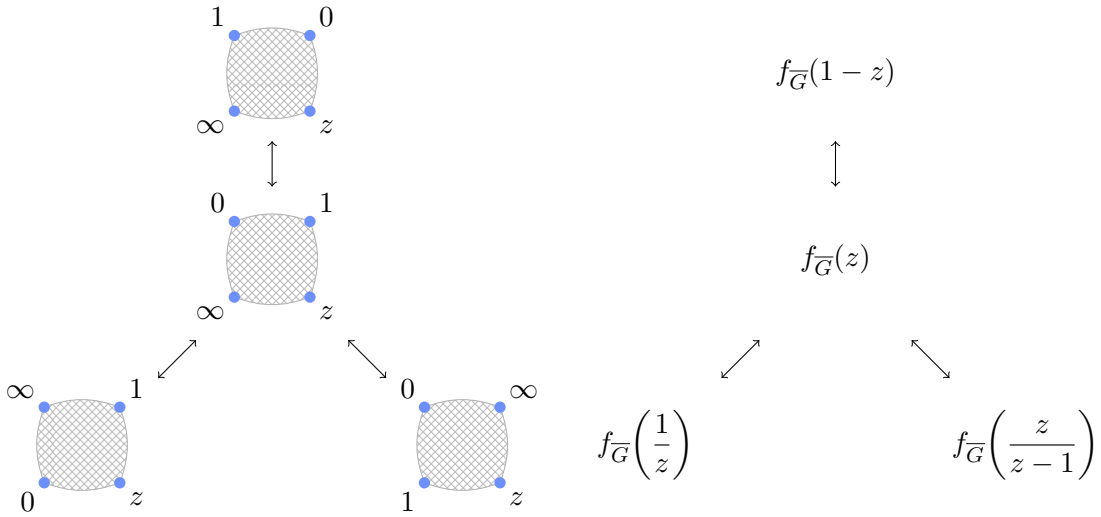

(3.14)

3.4 Ladder Graphs in Position Space

One of the main examples of the method of graphical functions discussed in [5] concerns a family of graphs known as the *generalised ladders*. It is not immediately obvious how these diagrams are related to the more familiar ladder Feynman diagrams in momentum space. In this section, we demonstrate that in four dimensions, the generalised ladders are in fact the position-space representations of the

usual four-point momentum-space ladder diagrams, as shown in Figure 3.1, following the argument of [18].

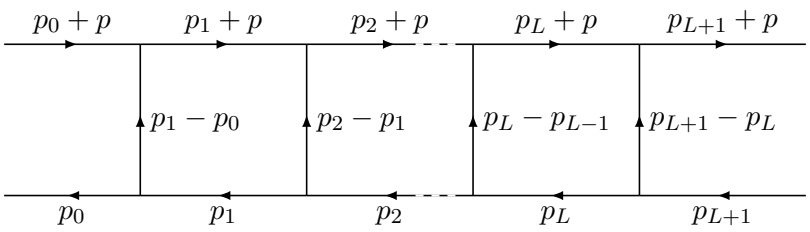

Figure 3.1: The four-point ladder diagram with L loops in momentum space.

In four dimensions, this diagram corresponds to the momentum-space integral

$$D_L(p_{L+1}, p_0, p) = \left(\prod_{k=1}^{L} \int \frac{d^4 p_k}{p_k^2 (p_k + p)^2}\right) \prod_{m=0}^{L} \frac{1}{(p_{m+1} - p_m)^2}. \tag{3.15}$$

This can be related to the position-space generalised ladder integral considered in [5] by applying the conformal transformation

$$p^\mu = \frac{x^\mu}{x^2}, \quad p_k^\mu = \frac{(x_k - x)^\mu}{(x_k - x)^2}. \tag{3.16}$$

Under this transformation, the metric for each x_k transforms as

$$\begin{aligned} g_{\alpha\beta} &= \eta_{\mu\nu} \frac{\partial p_k^\mu}{\partial x_k^\alpha} \frac{\partial p_k^\nu}{\partial x_k^\beta} = \eta_{\mu\nu} \frac{1}{[(x_k - x)^2]^2} \left(\delta_\alpha^\mu - 2\frac{(x_k - x)^\mu (x_k - x)^\alpha}{(x_k - x)^2}\right) \left(\delta_\beta^\nu - 2\frac{(x_k - x)^\nu (x_k - x)^\beta}{(x_k - x)^2}\right) \\ &= \frac{\eta_{\alpha\beta}}{[(x_k - x)^2]^2}, \end{aligned} \tag{3.17}$$

where $\eta_{\alpha\beta}$ is the usual Minkowski metric. Thus the transformed metric is related to the original metric by an overall factor, so the transformation is indeed conformal.

We now want to find the transformed form of the integral (3.15). Firstly, we note that the volume form transforms as

$$d^4 p_k = \sqrt{|g|}\, d^4 x_k = \frac{d^4 x_k}{[(x_k - x)^2]^4}, \tag{3.18}$$

where g denotes the determinant of the metric $g_{\alpha\beta}$. Next, we compute the transformed forms of the remaining expressions,

$$\begin{aligned} (p_{m+1} - p_m)^2 &= p_{m+1}^2 + p_m^2 - 2 p_{m+1} \cdot p_m \\ &= \frac{1}{(x_{m+1} - x)^2} + \frac{1}{(x_m - x)^2} - \frac{2(x_{m+1} - x) \cdot (x_m - x)}{(x_{m+1} - x)^2 (x_m - x)^2} \\ &= \frac{(x_{m+1} - x_m)^2}{(x_{m+1} - x)^2 (x_m - x)^2}, \end{aligned} \tag{3.19}$$

and

$$\begin{aligned} p_k^2 (p_k + p)^2 &= \frac{1}{(x_k - x)^2} \left(p_k^2 + p^2 + 2 p_k \cdot p\right) \\ &= \frac{1}{(x_k - x)^2} \left(\frac{1}{(x_k - x)^2} + \frac{1}{x^2} + \frac{2(x_k - x) \cdot x}{x^2 (x_k - x)^2}\right) \\ &= \frac{x_k^2}{x^2 [(x_k - x)^2]^2}. \end{aligned} \tag{3.20}$$

Combining these results, we see that the transformed form of (3.15) is

$$D_L(p_{L+1},p_0,p) = \left(\prod_{k=1}^{L}\int \frac{x^2\,d^4x_k}{x_k^2[(x_k-x)^2]^2}\right)\prod_{m=0}^{L}\frac{(x_{m+1}-x)^2(x_m-x)^2}{(x_{m+1}-x_m)^2}$$
$$= x^{2L}(x_0-x)^2(x_{L+1}-x)^2\left(\prod_{k=1}^{L}\int\frac{d^4x_k}{x_k^2}\right)\prod_{m=0}^{L}\frac{1}{(x_{m+1}-x_m)^2}. \tag{3.21}$$

We thus obtain the relation

$$p_{L+1}^2p_0^2(p^2/\pi^2)^L D_L(p_{L+1},p_0,p) = P_L(x_0,x_{L+1}), \tag{3.22}$$

where we have defined the integral

$$P_L(x_0,x_{L+1}) = \left(\prod_{k=1}^{L}\int\frac{d^4x_k}{\pi^2x_k^2}\right)\prod_{m=0}^{L}\frac{1}{(x_{m+1}-x_m)^2}. \tag{3.23}$$

Interpreting the transformed variables in position space, this integral corresponds to the diagram shown in Figure 3.2, which is precisely the generalised ladder diagram considered in [5]. Physically, this diagram corresponds to propagation from x_0 to x_{L+1}, with L interactions traced back to the origin O [18].

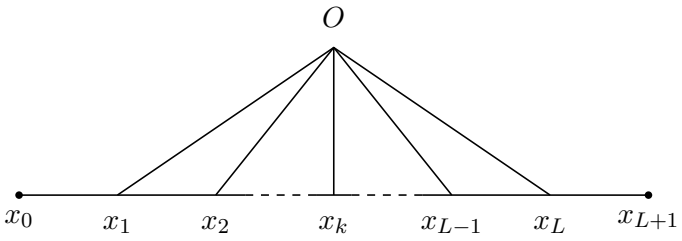

Figure 3.2: The four-point ladder diagram in position space.

We can also observe this relationship from a slightly different perspective. Figure 3.3 shows the dual graph of the momentum-space four-point ladder diagram, which corresponds to the position-space representation. Since each internal vertex of the dual graph has degree four, the corresponding integral is conformally invariant. This means that no information is lost if the point P is sent to infinity, whereupon we obtain the position-space graph shown in Figure 3.2 [19].

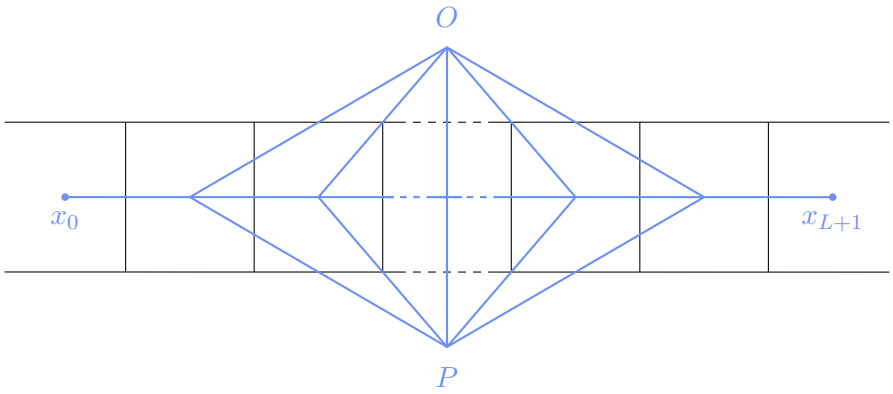

Figure 3.3: The position-space dual of the four-point ladder diagram.

By shrinking the final rung of the L-loop four-point ladder diagram to a point, we obtain the L-loop three-point ladder diagram, which is shown in Figure 3.4. The corresponding integral in momentum

space is

$$C_L(p_0,p)=\left(\prod_{k=1}^{L}\int\frac{d^4p_k}{p_k^2(p_k+p)^2}\right)\prod_{m=0}^{L-1}\frac{1}{(p_{m+1}-p_m)^2}, \tag{3.24}$$

which is related to the position-space integral (3.23) according to

$$p_0^2(p^2/\pi^2)^L C_L(p_0,p)=P_L(x_0,x). \tag{3.25}$$

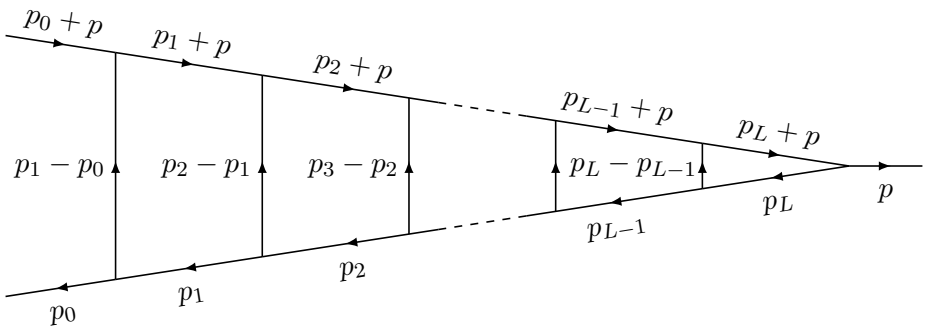

Figure 3.4: The three-point ladder diagram with L loops in momentum space.

The ladder diagrams provide interesting test cases for the development of new diagrammatic coaction formulae. In particular, the three-point ladder diagram with two loops will form a major focus of the following chapter.

4

The Diagrammatic Coaction Beyond One Loop

As discussed in Chapter 2, the diagrammatic coaction of one-loop Feynman integrals as formulated in [2, 3] is well understood. However, the diagrammatic coaction has not yet been fully generalised to multi-loop Feynman integrals. In [4], the first steps towards such a generalisation were taken, and diagrammatic coaction formulae were obtained for several two-loop examples, including the sunset integral, the double-edged triangle, and the adjacent triangle diagram.

In this chapter, we consider a different example of a two-loop Feynman integral: the two-loop three-point ladder. We compute the coaction on the relevant pure function in terms of multiple polylogarithms, and explore the possibility of finding a diagrammatic representation of this coaction. This exploration includes the reduction of the ladder to a linear combination of master integrals, and the computation of five of the relevant cuts of the ladder, two of which are found to vanish. We conclude the chapter by discussing why the sixth cut integral is more challenging to evaluate, and suggest several possible ways in which this calculation could be performed in future.

4.1 The Two-Loop Three-Point Ladder

The momentum-space Feynman diagram for the two-loop three-point ladder with massless propagators and three external scales p_1^2, p_2^2, p_3^2 is shown in Figure 4.1. There are several reasons for focusing on this diagram in particular, including that it is finite in four dimensions, that it evaluates to a function of multiple polylogarithms, and that it forms part of a large, well-studied family of three-point ladder diagrams with an arbitrary number of loops, as we saw in the previous chapter.

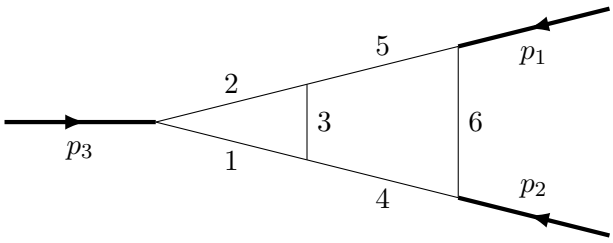

Figure 4.1: The two-loop three-point ladder diagram in momentum space.

In four dimensions, the Feynman integrals corresponding to three- and four-point ladder diagrams with an arbitrary number of rungs were first evaluated in [20]. In the case we are considering, the

integral in $D = 4 - 2\epsilon$ dimensions evaluates to

$$\begin{aligned} T_L(p_1^2, p_2^2, p_3^2) &= \left(\frac{e^{\gamma_{\nu_E}\epsilon}}{i\pi^{D/2}}\right)^2 \int d^D k \int d^D l \, \frac{1}{k^2(k-p_3)^2(l-k)^2 l^2 (l-p_3)^2 (k+p_1)^2} \\ &= i(p_1^2)^{-2} \frac{1}{(1-z)(1-\bar{z})(z-\bar{z})} F(z,\bar{z}) + \mathcal{O}(\epsilon), \end{aligned} \tag{4.1}$$

where we have defined the pure function

$$F(z,\bar{z}) = 6[\mathrm{Li}_4(z) - \mathrm{Li}_4(\bar{z})] - 3\log(z\bar{z})[\mathrm{Li}_3(z) - \mathrm{Li}_3(\bar{z})] + \frac{1}{2}\log^2(z\bar{z})[\mathrm{Li}_2(z) - \mathrm{Li}_2(\bar{z})], \tag{4.2}$$

with arguments z and $\bar{z}$ defined in terms of the external momenta as in (1.46). To compute the components of the coaction on this function, we use the formula (1.25) for the coaction on the classical polylogarithms to obtain

$$\begin{aligned} \Delta_{1,3}[F(z,\bar{z})] &= \log(z\bar{z}) \otimes \big[-3\,\mathrm{Li}_3(z) + 3\,\mathrm{Li}_3(\bar{z}) + \log(z\bar{z})\big(\mathrm{Li}_2(z) - \mathrm{Li}_2(\bar{z})\big)\big] \\ &\quad + \log\big((1-z)(1-\bar{z})\big) \otimes \frac{1}{2}\log z \log\bar{z} \log\frac{z}{\bar{z}}, \end{aligned} \tag{4.3a}$$

$$\begin{aligned} \Delta_{2,2}[F(z,\bar{z})] &= \big[\mathrm{Li}_2(z) - \mathrm{Li}_2(\bar{z}) + \log(1-z)\log(z\bar{z})\big] \otimes \frac{1}{2}\big[\log^2 z - 2\log z \log\bar{z}\big] \\ &\quad + \big[\mathrm{Li}_2(z) - \mathrm{Li}_2(\bar{z}) - \log(1-\bar{z})\log(z\bar{z})\big] \otimes \frac{1}{2}\big[\log^2\bar{z} - 2\log z\log\bar{z}\big] \\ &\quad + \frac{1}{2}\log^2(z\bar{z}) \otimes [\mathrm{Li}_2(z) - \mathrm{Li}_2(\bar{z})], \end{aligned} \tag{4.3b}$$

$$\begin{aligned} \Delta_{3,1}[F(z,\bar{z})] &= \big[3\,\mathrm{Li}_3(z) + 3\,\mathrm{Li}_3(\bar{z}) - \log(z\bar{z})\big(\mathrm{Li}_2(z) - \mathrm{Li}_2(\bar{z})\big)\big] \otimes \log\frac{z}{\bar{z}} \\ &\quad - \frac{1}{2}\log(z\bar{z})\big[2\,\mathrm{Li}_2(z) + \log(1-z)\log(z\bar{z})\big] \otimes \log z \\ &\quad + \frac{1}{2}\log(z\bar{z})\big[2\,\mathrm{Li}_2(\bar{z}) + \log(1-\bar{z})\log(z\bar{z})\big] \otimes \log\bar{z}, \end{aligned} \tag{4.3c}$$

in agreement with the results of [11].

To obtain a formula for the diagrammatic coaction of the two-loop three-point ladder, we would need to find a way of expressing the above coaction in terms of Feynman integrals and cut Feynman integrals. It is worthwhile to pause to consider the form that such a diagrammatic coaction is expected to take. As discussed in [4], any diagrammatic coaction on an L-loop integral should be expressible in terms of integrals with L loops. This indicates that the diagrammatic coaction of our ladder diagram should have a representation in terms of two-loop integrals.

We also note that the two-loop three-point ladder is *reducible*, which means that it can be expressed as a linear combination of integrals with fewer propagators. Based on the arguments in [4], we expect that the ladder itself will not appear in the left entries of its diagrammatic coaction, and that its maximal cut will vanish, while its non-maximal cuts will appear in the right entries.

Moreover, we saw in Chapter 3 that the L-loop three-point ladder diagram is dual conformally invariant; that is, that the integral represented by the dual diagram is conformally invariant. In [2], it was shown that the coaction on dual conformally invariant one-loop Feynman integrals can be expressed entirely in terms of integrals which are themselves dual conformally invariant. It is therefore of interest to consider whether this property continues to hold for the diagrammatic coaction on the two-loop three-point ladder, and this could potentially serve as a guiding principle when attempting to determine the terms in the coaction.

4.2 Reduction to Master Integrals

We now wish to express the left entries of the above coaction components (4.3) in terms of the two-loop master integrals of the original diagram, and the right entries in terms of cuts of the original diagram. A logical step towards this goal is to reduce the ladder to a linear combination of master integrals via integration-by-parts relations.

The topology of the two-loop three-point ladder diagram in D dimensions is defined by the set of integrals of the form

$$\begin{aligned} &I(\nu_1,\nu_2,\nu_3,\nu_4,\nu_5,\nu_6,\nu_7;D;p_1^2,p_2^2,p_3^2) \\ &\quad= \left(\frac{e^{\gamma_E\epsilon}}{i\pi^{D/2}}\right)^2 \int d^Dk \int d^Dl \, \frac{[(l+p_1)^2]^{-\nu_7}}{[k^2]^{\nu_1}[(k-p_3)^2]^{\nu_2}[(l-k)^2]^{\nu_3}[l^2]^{\nu_4}[(l-p_3)^2]^{\nu_5}[(k+p_1)^2]^{\nu_6}} \end{aligned} \tag{4.4}$$

for integer ν_i with $\nu_7 \leq 0$. Comparing this expression with (4.1), we see that the two-loop three-point ladder diagram is given by $I(1,1,1,1,1,1,0)$, where we suppress the final four arguments when the dependence on the spacetime dimension D and the external momenta is obvious. The numerator with exponent ν_7 has been added to extend the set of propagators to a basis for the topology.

Using the Mathematica package `FIRE` [21], we obtain the following integration-by-parts reduction formula for the two-loop three-point ladder diagram in $D = 4 - 2\epsilon$ dimensions:

$$\begin{aligned} I(1,1,1,1,1,1,0) = \frac{1}{p_3^2}\Big(&\frac{1}{\epsilon}I(1,1,2,0,0,1,0) - \frac{1}{\epsilon}I(0,1,2,1,0,1,0) - \frac{1}{\epsilon}I(1,0,2,0,1,1,0) \\ &-I(1,1,1,1,0,1,0) - I(1,1,1,0,1,1,0) - \frac{(1-2\epsilon)}{\epsilon}I(1,1,0,1,1,1,0)\Big). \end{aligned} \tag{4.5}$$

This reduction formula expresses the original six-propagator ladder integral as a linear combination of basis integrals with fewer propagators; these basis integrals are known as *master integrals* [6]. In diagram form, this formula can be expressed as

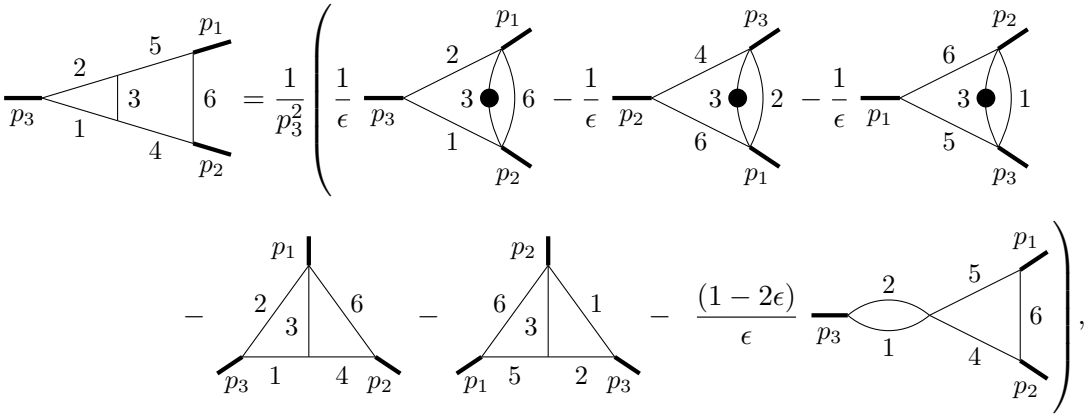

(4.6)

where the dots denote squared propagators. We thus see that the ladder can be expressed in terms of six master integrals: three double-edged triangles with squared propagators, two adjacent triangle diagrams, and one product of a bubble with a triangle. We expect these master integrals to appear in the first entries of the diagrammatic coaction, and their corresponding cut integrals to appear in the second entries.

The leading-order coefficients of the Laurent series expansions of these master integrals in the dimensional regulator are well known in the literature. The double-edged triangle with squared propagator is given to all orders in ϵ in terms of Appell F_4 functions in [4]. The leading order result for the adjacent triangle diagram can be found in [22]. Finally, the bubble-triangle product diagram is trivially computed by taking the product of the functions corresponding to the bubble integral and triangle integral, whose expansions can be found in [2].

4.3 Computation of Cut Integrals

We now turn to the elements which are expected to form the second entries of the diagrammatic coaction of the two-loop three-point ladder: the cuts of this diagram. Cuts of one-loop Feynman integrals were discussed in Chapter 1, where we saw that they can be defined using either the Dirac delta function prescription (1.33), or the residue prescription (1.36). We must now consider the generalisation of the operation of cutting propagators to the multi-loop case. There are several different notions of cuts which appear in the literature, including *unitarity cuts* and *generalised cuts*; the various definitions are reviewed in [23]. Here, we will compute the relevant cut integrals via the loop-by-loop approach, as described in [4], where we impose the cut conditions using the delta function prescription (1.33).

The relevant cut diagrams may be determined by considering the master integrals found above for the two-loop three-point ladder. For each master integral, we obtain a corresponding cut of the ladder diagram, where the set of cut propagators is precisely the set of propagators which occur in that master integral. Following this procedure for the six master integrals above, we obtain the cut diagrams shown in Figure 4.2.

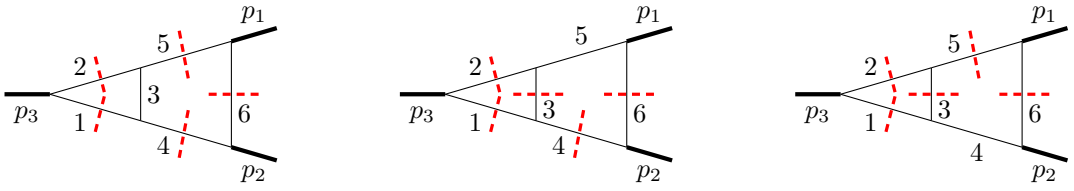

(a) $\mathcal{C}_{1,2,4,5,6}T_L$ (b) $\mathcal{C}_{1,2,3,4,6}T_L$ (c) $\mathcal{C}_{1,2,3,5,6}T_L$

(d) $\mathcal{C}_{2,3,4,6}T_L$ (e) $\mathcal{C}_{1,3,5,6}T_L$ (f) $\mathcal{C}_{1,2,3,6}T_L$

Figure 4.2: The cut integrals corresponding to the master integrals of the two-loop three-point ladder, which are expected to appear in the right entries of the diagrammatic coaction.

These cut integrals are expected to appear in the second entries of the diagrammatic coaction of the ladder, paired with first entries consisting of the corresponding master integrals. As the Laurent series expansions of the master integrals in the dimensional regulator ϵ are already known, the remaining task is to evaluate the series expansions of the cut integrals.

In the remainder of this section, we evaluate the first five cut integrals of Figure 4.2, and discuss why the sixth integral is particularly challenging to compute. The calculations are performed using a loop-by-loop approach, as described in [4]; this involves evaluating the two-loop integral by first integrating over a one-loop subdiagram. We impose cuts of propagators using the delta function prescription (1.33). For simplicity, we suppress factors of $e^{\gamma_E \epsilon}$ throughout.

4.3.1 Five-Propagator Cuts

Cut (a) We will start by considering the next-to-maximal cuts, beginning with the cut shown in Figure 4.2a. Taking a loop-by-loop approach, we choose to integrate over the triangle subdiagram first. We thus express the cut integral as

$$\mathcal{C}_{1,2,4,5,6}T_L(p_1^2,p_2^2,p_3^2) = \mathcal{C}_{4,5,6}\int \frac{d^Dk}{i\pi^{D/2}} \frac{1}{k^2(k-p_3)^2(k+p_1)^2} \mathcal{C}_{1,2} \int \frac{d^Dl}{i\pi^{D/2}} \frac{1}{l^2(l-p_3)^2(k-l)^2}. \quad (4.7)$$

Using the result for the two-propagator cut of the triangle integral with three external masses from [2], we have

$$\mathcal{C}_{1,2}\int\frac{d^Dl}{i\pi^{D/2}}\frac{1}{l^2(l-p_3)^2(k-l)^2}=\frac{\Gamma(1-\epsilon)}{\epsilon\Gamma(1-2\epsilon)}\frac{(p_3^2)^{-\epsilon}}{(k-p_3)^2-p_3^2}, \tag{4.8}$$

which can be substituted into the full integral above to obtain

$$\mathcal{C}_{1,2,4,5,6}T_L=-i\pi^{-2+\epsilon}\frac{\Gamma(1-\epsilon)}{\epsilon\Gamma(1-2\epsilon)}(p_3^2)^{-\epsilon}\int d^{4-2\epsilon}k\frac{(-2\pi i)^3\delta(k^2)\delta((k-p_3)^2)\delta((k+p_1)^2)}{(k-p_3)^2-p_3^2}. \tag{4.9}$$

To evaluate the remaining integral, we introduce the parameterisation

$$p_1=\sqrt{p_1^2}(1,\mathbf{0}_{3-2\epsilon}),\quad p_3=\sqrt{p_3^2}(\alpha,\sqrt{\alpha^2-1},\mathbf{0}_{2-2\epsilon}),\quad k=k_0(1,\beta\cos\theta,\beta\sin\theta\mathbf{1}_{2-2\epsilon}), \tag{4.10}$$

where $\mathbf{1}_{2-2\epsilon}$ ranges over unit vectors in the dimension transverse to the external momenta, and the value of α is fixed by momentum conservation to be

$$\alpha=\frac{p_2^2-p_1^2-p_3^2}{2\sqrt{p_1^2}\sqrt{p_3^2}}. \tag{4.11}$$

This parameterisation results in the integration measure

$$\int d^{4-2\epsilon}k=\frac{2\pi^{1-\epsilon}}{\Gamma(1-\epsilon)}\int_{-\infty}^{+\infty}dk_0\,k_0^{3-2\epsilon}\int_0^{\infty}d\beta\,\beta^{2-2\epsilon}\int_0^{\pi}d\theta\sin^{1-2\epsilon}\theta, \tag{4.12}$$

and we also obtain $k^2=k_0^2(1-\beta^2)$. Noting that $\beta>0$ by definition, we have

$$\delta(k^2)=\delta(k_0^2(1-\beta^2))=\frac{1}{2\beta k_0^2}\delta(\beta-1), \tag{4.13}$$

so that the cut condition $k^2=0$ is imposed by evaluating the residue at $\beta=1$. The remaining cut propagators can be expressed as

$$\begin{aligned}(k+p_1)^2&=k_0^2(1-\beta^2)+p_1^2+2k_0\sqrt{p_1^2},\\(k-p_3)^2&=k_0^2(1-\beta^2)+p_3^2-2k_0\sqrt{p_3^2}(\alpha-\beta\sqrt{\alpha^2-1}\cos\theta),\end{aligned} \tag{4.14}$$

so that, upon taking the residue at $\beta=1$, the cut integral becomes

$$\begin{aligned}\mathcal{C}_{1,2,4,5,6}T_L&=-\frac{8\pi^2}{\epsilon\Gamma(1-2\epsilon)}(p_3^2)^{-\epsilon}\int_{-\infty}^{+\infty}dk_0\,k_0^{1-2\epsilon}\int_0^{\pi}d\theta\sin^{1-2\epsilon}\theta\\&\quad\times\frac{\delta\Big(p_3^2-2k_0\sqrt{p_3^2}(\alpha-\sqrt{\alpha^2-1}\cos\theta)\Big)\delta\Big(p_1^2+2k_0\sqrt{p_1^2}\Big)}{-2k_0\sqrt{p_3^2}(\alpha-\sqrt{\alpha^2-1}\cos\theta)}\\&=\frac{2^{2+2\epsilon}\pi^2}{\epsilon\Gamma(1-2\epsilon)}(p_3^2)^{-\epsilon}(p_1^2)^{-1-\epsilon}\int_0^{\pi}d\theta\sin^{1-2\epsilon}\theta\frac{\delta\Big(p_3^2+\sqrt{p_1^2}\sqrt{p_3^2}(\alpha-\sqrt{\alpha^2-1}\cos\theta)\Big)}{\sqrt{p_1^2}\sqrt{p_3^2}(\alpha-\sqrt{\alpha^2-1}\cos\theta)}.\end{aligned} \tag{4.15}$$

We now perform the change of variables

$$\cos\theta=2x-1,\quad x\in[0,1], \tag{4.16}$$

which gives the measure

$$\int_0^{\pi}d\theta\sin^{1-2\epsilon}\theta=2^{1-2\epsilon}\int_0^1dx\,x^{-\epsilon}(1-x)^{-\epsilon}. \tag{4.17}$$

This allows us to use the remaining delta function to perform the final integral over x. Upon introducing the variables z and $\bar{z}$ defined by (1.46), this yields the result

$$\begin{aligned}\mathcal{C}_{1,2,4,5,6}T_L &= -\frac{8\pi^2}{\epsilon\Gamma(1-2\epsilon)}(p_3^2)^{-1-\epsilon}(p_1^2)^{-1-\epsilon}\int_0^1 dx\, x^{-\epsilon}(1-x)^{-\epsilon}\frac{\delta\left(x+\frac{(1-z)\bar{z}}{z-\bar{z}}\right)}{(z-\bar{z})(1-z+(z-\bar{z})x)}\\ &= \frac{8\pi^2}{\epsilon\Gamma(1-2\epsilon)}\frac{(p_1^2)^{-2-2\epsilon}}{(1-z)(1-\bar{z})(z-\bar{z})}\left(\frac{(z-\bar{z})^2}{z\bar{z}(1-z)^2(1-\bar{z})^2}\right)^{\epsilon}.\end{aligned} \tag{4.18}$$

Clearly, the series expansion of this expression in ϵ can easily be computed in terms of logarithms to arbitrary order.

Cut (b) We now move on to the cut diagram shown in Figure 4.2b. Again choosing to start with the triangle subloop, we express the cut integral as

$$\mathcal{C}_{1,2,3,4,6}T_L(p_1^2,p_2^2,p_3^2) = \mathcal{C}_{5,6}\int\frac{d^Dk}{i\pi^{D/2}}\frac{1}{k^2(k-p_3)^2(k+p_1)^2}\mathcal{C}_{1,2,3}\int\frac{d^Dl}{i\pi^{D/2}}\frac{1}{l^2(l-p_3)^2(k-l)^2}. \tag{4.19}$$

Using the result for the maximal cut of the three-mass triangle from [2], we obtain

$$\begin{aligned}&C_{1,2,3}\int\frac{d^Dl}{i\pi^{D/2}}\frac{1}{l^2(l-p_3)^2(k-l)^2}\\ &\quad= -\frac{(p_3^2)^{-\epsilon}}{\Gamma(1-\epsilon)}\left(k^2\right)^{-\epsilon}\left((k-p_3)^2\right)^{-\epsilon}\left[(k^2-p_3^2)^2-2(k^2+p_3^2)(k-p_3)^2+(k-p_3)^2\right].\end{aligned} \tag{4.20}$$

We immediately see that when we impose the cut condition on propagator 5 using the delta function $\delta(k^2)$, this expression will evaluate to zero, which implies that this cut diagram vanishes.

Cut (c) By the symmetry of this diagram and the previous one under the transformation $p_1 \leftrightarrow p_2$, the cut integral $\mathcal{C}_{1,2,3,5,6}T_L$ shown in Figure 4.2c also vanishes.

4.3.2 Four-Propagator Cuts

Cut (d) The next case to be evaluated is the four-propagator cut shown in Figure 4.2d. We again choose to integrate over the triangle subdiagram first, so we express the cut integral as

$$\mathcal{C}_{2,3,4,6}T_L = \mathcal{C}_{4,6}\int\frac{d^Dk}{i\pi^{D/2}}\frac{1}{k^2(k-p_3)^2(k+p_1)^2}\mathcal{C}_{1,3}\int\frac{d^Dl}{i\pi^{D/2}}\frac{1}{l^2(l-p_3)^2(k-l)^2}. \tag{4.21}$$

Again using the result for the two-propagator cut of the triangle integral with three external masses from [2], we have

$$\mathcal{C}_{1,3}\int\frac{d^Dl}{i\pi^{D/2}}\frac{1}{l^2(l-p_3)^2(k-l)^2} = -\frac{\Gamma(1-\epsilon)}{\epsilon\Gamma(1-2\epsilon)}\frac{\left((k-p_3)^2\right)^{-\epsilon}}{(k-p_3)^2-p_3^2}. \tag{4.22}$$

Substituting this into the expression for the full cut integral, we obtain

$$\mathcal{C}_{2,3,4,6}T_L = i\pi^{-2+\epsilon}\frac{\Gamma(1-\epsilon)}{\epsilon\Gamma(1-2\epsilon)}\int d^{4-2\epsilon}k\frac{(-2\pi i)^2\delta(k^2)\delta((k+p_1)^2)}{\left((k-p_3)^2\right)^{1+\epsilon}\left((k-p_3)^2-p_3^2\right)}. \tag{4.23}$$

Introducing the parameterisation (4.10) and integrating over β as before, we obtain

$$\begin{aligned}\mathcal{C}_{2,3,4,6}T_L &= \frac{4\pi i}{\epsilon\Gamma(1-2\epsilon)}\int_{-\infty}^{+\infty} dk_0\, k_0^{1-2\epsilon}\int_0^{\pi} d\theta \sin^{1-2\epsilon}\theta\,\delta\big(p_1^2+2\sqrt{p_1^2}k_0\big)\\ &\quad\times\Big(p_3^2-2k_0\sqrt{p_3^2}(\alpha-\sqrt{\alpha^2-1}\cos\theta)\Big)^{-1-\epsilon}\Big(-2k_0\sqrt{p_3^2}(\alpha-\sqrt{\alpha^2-1})\cos\theta\Big)^{-1}\\ &= \frac{2^{2\epsilon}\pi i}{\epsilon\Gamma(1-2\epsilon)}(p_1^2)^{-\epsilon}\int_0^{\pi} d\theta\sin^{1-2\epsilon}\theta\Big(p_3^2+\sqrt{p_1^2}\sqrt{p_3^2}(\alpha-\sqrt{\alpha^2-1}\cos\theta)\Big)^{-1-\epsilon}\\ &\quad\times\Big(\sqrt{p_1^2}\sqrt{p_3^2}(\alpha-\sqrt{\alpha^2-1}\cos\theta)\Big)^{-1}. \end{aligned}\tag{4.24}$$

As before, we now introduce the variable x defined by (4.16), and the variables z and $\bar{z}$ defined by (1.46). This yields the final result

$$\begin{aligned}\mathcal{C}_{2,3,4,6}T_L &= \frac{2\pi i}{\epsilon\Gamma(1-2\epsilon)}(p_1^2)^{-2-2\epsilon}((1-z)\bar{z})^{-1-\epsilon}(1-z)^{-1}\\ &\quad\times\int_0^1 dx\, x^{-\epsilon}(1-x)^{-\epsilon}\Big(1+\frac{z-\bar{z}}{(1-z)\bar{z}}x\Big)^{-1-\epsilon}\Big(1+\frac{z-\bar{z}}{1-z}x\Big)^{-1}\\ &= \frac{1-2\epsilon}{\epsilon}\frac{2\pi i}{\Gamma^2(1-\epsilon)}\frac{(p_1^2)^{-2-2\epsilon}}{(1-z)^{2+\epsilon}\bar{z}^{1+\epsilon}}F_1\Big(1-\epsilon;1+\epsilon,1;2-2\epsilon;-\frac{z-\bar{z}}{(1-z)\bar{z}},-\frac{z-\bar{z}}{1-z}\Big), \end{aligned}\tag{4.25}$$

where we have expressed the result in terms of the Appell F_1 function, which is a hypergeometric series of two variables with the integral representation [6]

$$F_1(\alpha;\beta,\beta';\gamma;x,y) = \frac{\Gamma(\gamma)}{\Gamma(\alpha)\Gamma(\gamma-\alpha)}\int_0^1 du\, u^{\alpha-1}(1-u)^{\gamma-\alpha-1}(1-ux)^{-\beta}(1-uy)^{-\beta'}.\tag{4.26}$$

This series expansion of the Appell F_1 function may be performed using the Mathematica package `MultiHypExp` [24], which is based on the algorithm described in [25].

Cut (e) The cut integral $\mathcal{C}_{2,3,5,6}T_L$ shown in Figure 4.2e can be obtained from the previous result simply by interchanging $p_1 \leftrightarrow p_2$.

Cut (f) Finally, we turn to the cut integral $\mathcal{C}_{1,2,3,6}T_L$, shown in Figure 4.2f, which we express as

$$\mathcal{C}_{1,2,3,6}T_L = \mathcal{C}_6\int\frac{d^Dk}{i\pi^{D/2}}\frac{1}{k^2(k-p_3)^2(k+p_1)^2}\mathcal{C}_{1,2,3}\int\frac{d^Dl}{i\pi^{D/2}}\frac{1}{l^2(l-p_3)^2(k-l)^2}.\tag{4.27}$$

Again using the expression (4.20) for the maximal cut of the triangle subdiagram, we obtain

$$\begin{aligned}\mathcal{C}_{1,2,3,6}T_L &= -i\pi^{-2+\epsilon}\frac{(p_3^2)^{-\epsilon}}{\Gamma(1-\epsilon)}\int d^{4-2\epsilon}k\frac{-2\pi i\delta\big((k+p_1)^2\big)}{(k^2)^{1+\epsilon}[(k-p_3)^2]^{1+\epsilon}}\\ &\quad\times\big[(k^2-p_3^2)^2-2(k^2+p_3^2)(k-p_3)^2+(k-p_3)^4\big]^{-\frac{1}{2}+\epsilon}. \end{aligned}\tag{4.28}$$

We note that, unlike in our other cut integrals, the exponent of one of the propagators here has the form $a+b\epsilon$ for non-integer a, which will ultimately make this integral substantially more challenging to evaluate using our current method. Nevertheless, we will press on with our current approach until the difficulty becomes manifest. To simplify the argument of the delta function, we first perform the shift $k \to k-p_1$, which gives

$$\begin{aligned}\mathcal{C}_{1,2,3,6}T_L &= -2\pi^{-1+\epsilon}\frac{(p_3^2)^{-\epsilon}}{\Gamma(1-\epsilon)}\int d^{4-2\epsilon}k\frac{\delta\big(k^2\big)}{[(k-p_1)^2]^{1+\epsilon}[(k+p_2)^2]^{1+\epsilon}}\\ &\quad\times\big[((k-p_1)^2-p_3^2)^2-2((k-p_1)^2+p_3^2)(k+p_2)^2+(k+p_2)^4\big]^{-\frac{1}{2}+\epsilon}. \end{aligned}\tag{4.29}$$

We now follow the same procedure as was used for the previous cut computations. We first introduce a parameterisation very similar to (4.10), except that now we replace p_3 with p_2, as the integral currently under consideration contains the quantity $(k+p_2)^2$ instead of the quantity $(k+p_1)^2$. We can then perform the integral over β using the delta function, and introduce the variable x defined by (4.16). This whole procedure ultimately leads to an integral of the form

$$\begin{aligned}\mathcal{C}_{1,2,3,6}T_L \sim \int dk_0\, k_0^{-2+\epsilon}\left(k_0-\frac{\sqrt{p_1^2}}{2}\right)^{-1-\epsilon}\int_0^1 dx\, x^{-\epsilon}(1-x)^{-\epsilon}\left(x+\frac{\left(2k_0-\sqrt{p_1^2}z\right)\bar{z}}{2k_0(z-\bar{z})}\right)^{-1-\epsilon}\\ \times\left(x-\frac{2k_0(1-\bar{z})+\sqrt{p_1^2}(z+\bar{z}-2)-2\sqrt{(1-z)(1-\bar{z})\left(p_1^2-2k_0\sqrt{p_1^2}\right)}}{2k_0(z-\bar{z})}\right)^{-\frac{1}{2}+\epsilon}\\ \times\left(x-\frac{2k_0(1-\bar{z})+\sqrt{p_1^2}(z+\bar{z}-2)+2\sqrt{(1-z)(1-\bar{z})\left(p_1^2-2k_0\sqrt{p_1^2}\right)}}{2k_0(z-\bar{z})}\right)^{-\frac{1}{2}+\epsilon},\end{aligned} \tag{4.30}$$

where we have suppressed prefactors which are independent of x and k_0. When faced with a complicated integral such as this, the most pragmatic approach is usually to perform a series expansion of the integrand in ϵ before integrating. When the factors in the integrand are raised to exponents of the form $a+b\epsilon$ for integer a and b, it is possible to write the coefficients of the Laurent expansion as linear combinations of multiple polylogarithms. The integration over the multiple polylogarithms may then be performed using the Mathematica package `PolyLogTools` [26]. However, the half-integers which appear in two of the exponents of this integrand mean that the Laurent coefficients cannot be directly expressed in terms of multiple polylogarithms in this case, so a different method is required.

Another important difference exhibited by this cut integral when compared to the previous cases considered here is that the cut conditions do not pick out a single value of k_0 which yields a nonzero result. The integration region over k_0 is not determined by the cut conditions, and the integral (4.30) may yield multiple independent cuts based on the choice of endpoints [4].

There are several approaches which could be explored in the attempt to evaluate this cut integral. In fact, the difficulty encountered here involving the appearance of square roots when starting with the maximal cut of a three-mass triangle was noted in [11], where the problem was circumvented by integrating first over the box subloop of the ladder, rather than starting with the triangle subloop. This is likely the most promising way to compute the integral while continuing to operate within the framework of our current loop-by-loop approach. Failing this, it may be possible to rationalise the square root via a well-chosen change of variables, in which case we could proceed to evaluate the integral (4.30). An algorithmic approach to finding such changes of variables can be found in [27].

Alternatively, it may be better to change our approach more fundamentally for this case, and try evaluating this cut integral via a different representation for Feynman integrals. In particular, the Baikov representation may be well-suited to this computation, as the operation of cutting a subset of propagators takes a particularly simple form in this representation [28], and may result in a simpler integral which can be evaluated to the required order in ϵ. Otherwise, the Mellin-Barnes representation could also be explored as another potential method of computing this cut; an overview of this technique can be found in [6]. Finally, it might be useful to consider the method of computing Feynman integrals via differential equations. The method of differential equations as applied to Feynman integrals is described in [29], and it is possible to adapt this approach to the computation of cut Feynman integrals. All of these options provide promising avenues for future exploration.

5

Conclusions

In this project, we have performed a detailed study of the coalgebra structure of Feynman integrals. Gaining a greater understanding of this structure is thought to be a promising route to the discovery of more efficient computational techniques for the evaluation of Feynman integrals, which is often a difficult task. Our particular focus has been the diagrammatic coaction of [2, 3], which realises the coaction on Feynman integrals in terms of operations performed on the corresponding graphs.

The foundation of this field of study is the coaction conjecture of [1], and in the earlier chapters of this report we discussed two different areas of research motivated by this principle. The first area was based on the study of the diagrammatic coaction, of which the one-loop formulation was discussed in some detail in Chapter 2. We saw that at one loop, the diagrammatic coaction is expressed as a linear combination of tensor products of Feynman graphs, where the first entries are pinched graphs and the second entries are cut graphs, and that there is a well-understood general rule for computing the diagrammatic coaction on any one-loop Feynman integral. The second approach considered here was the method of graphical functions as set forth in [5]. Graphical functions are massless three-point Feynman integrals parameterised to be functions on the complex plane, and one of their major advantages is that they may be built up recursively from trivial base graphs using a set of transformation rules. As discussed in Chapter 3, computations carried out using this method have provided more evidence in support of the coaction conjecture. At the end of this chapter, we also introduced the families of three- and four-point ladder diagrams, and discussed their properties of dual conformal invariance.

As we saw in Chapter 2, the diagrammatic coaction at one-loop is well-understood. However, it has not yet been fully generalised to the multi-loop case, and the primary focus of this project was an exploration of the diagrammatic coaction of the two-loop three-point ladder diagram. The main results of this study were contained in Chapter 4. These included the reduction of the ladder diagram to a linear combination of master integrals, of which there were found to be six: three double-edged triangles, two adjacent triangle diagrams, and one bubble-triangle product diagram. The cut of the ladder corresponding to each of these master integrals was determined. Two of these cuts were found to vanish, and three of the others were computed to all orders in ϵ using the loop-by-loop approach of [4]. The final cut integral remains unevaluated, as the complexity of its structure presented a significant challenge when using the loop-by-loop approach. The evaluation of this integral would be the obvious next step in any future attempt to extend this work.

We conclude this report by considering possible avenues for extending the work presented here. While progress was made towards gaining a greater understanding of the potential structure of the diagrammatic coaction of the two-loop three-point ladder diagram, the precise form of this coaction remains to be determined. The next step towards formulating such an expression for the coaction would clearly be to evaluate the last remaining unevaluated cut integral. We observed here that the loop-by-loop approach resulted in a highly complicated expression at an intermediate stage of the calculation when the triangle subloop was integrated over first, and that the emergence of square roots meant that we could not immediately apply computational tools developed for multiple polylogarithms. The calculation may be simplified if one instead chooses to integrate first over the box subloop, and this seems to be the most promising way in which the cut integral could be evaluated in future.

Alternatively, it may prove fruitful to try evaluating the integral via other methods; in particular, the Baikov formalism may provide a more tractable approach.

Once this integral has been evaluated, all of the components which are expected to appear in the diagrammatic coaction will be known, and may be expressed as Laurent series in the dimensional regulator. The task will then be to compare these expressions to the known coaction of the two-loop three-point ladder in terms of multiple polylogarithms, with the aim of finding an arrangement such that the first entries correspond to the master integrals of the ladder, while the second entries correspond to the associated cut integrals. It may initially prove easier to consider the expressions for each diagram on the level of the symbol, which is the maximal iteration of the coaction. While some information will be lost by taking this approach, the expressions will be greatly simplified and this is likely to facilitate the identification of possible forms that the full diagrammatic coaction may take.

Obtaining a diagrammatic representation of the coaction on the two-loop three-point ladder would provide a new example of the diagrammatic coaction on a multi-loop Feynman integral, in addition to those considered using the interpretation of the integrals in terms of hypergeometric functions in [4]. Such an example would be interesting in light of the fact that the complete generalisation of the diagrammatic coaction to the multi-loop case is yet to be determined.

Bibliography

[1] F. Brown. 'Feynman amplitudes, coaction principle, and cosmic Galois group'. *Communications in Number Theory and Physics* 11 (2017), pp. 453–556. arXiv: 1512.06409 [math-ph].

[2] S. Abreu, R. Britto, C. Duhr and E. Gardi. 'Diagrammatic Hopf algebra of cut Feynman integrals: the one-loop case'. *Journal of High Energy Physics* 2017.12 (2017). arXiv: 1704.07931v2 [hep-th].

[3] S. Abreu, R. Britto, C. Duhr and E. Gardi. 'Algebraic Structure of Cut Feynman Integrals and the Diagrammatic Coaction'. *Physical Review Letters* 119 (5 2017), p. 051601. arXiv: 1703.05064 [hep-th].

[4] S. Abreu, R. Britto, C. Duhr, E. Gardi and J. Matthew. 'The diagrammatic coaction beyond one loop'. *Journal of High Energy Physics* 2021.10 (2021). arXiv: 2106.01280 [hep-th].

[5] M. Borinsky and O. Schnetz. 'Recursive computation of Feynman periods'. *Journal of High Energy Physics* 2022.8 (2022), p. 291. arXiv: 2206.10460v2 [hep-th].

[6] S. Weinzierl. *Feynman Integrals*. Springer, 2022. arXiv: 2201.03593 [hep-th].

[7] R. E. Cutkosky. 'Singularities and Discontinuities of Feynman Amplitudes'. *Journal of Mathematical Physics* 1.5 (1960), pp. 429–433.

[8] S. Abreu, R. Britto, C. Duhr and E. Gardi. 'Cuts from residues: the one-loop case'. *Journal of High Energy Physics* 2017.6 (2017). arXiv: 1702.03163 [hep-th].

[9] K. J. Larsen and Y. Zhang. 'Integration-by-parts reductions from unitarity cuts and algebraic geometry'. *Physical Review D* 93.4 (2016). arXiv: 1511.01071 [hep-th].

[10] A. Primo and L. Tancredi. 'On the maximal cut of Feynman integrals and the solution of their differential equations'. *Nuclear Physics B* 916 (2017), pp. 94–116. arXiv: 1610.08397 [hep-th].

[11] S. Abreu, R. Britto, C. Duhr and E. Gardi. 'From multiple unitarity cuts to the coproduct of Feynman integrals'. *Journal of High Energy Physics* 2014.10 (2014). arXiv: 1401.3546 [hep-th].

[12] S. Abreu, R. Britto, C. Duhr, E. Gardi and J. Matthew. 'From positive geometries to a coaction on hypergeometric functions'. *Journal of High Energy Physics* 2020.2 (2020). arXiv: 1910.08358 [hep-th].

[13] G. 't Hooft. 'Dimensional regularization and the renormalization group'. *Nuclear Physics B* 61 (1973), pp. 455–468.

[14] T. Y. Semenova, A. V. Smirnov and V. A. Smirnov. 'On the status of expansion by regions'. *The European Physical Journal C* 79.2 (2019). arXiv: 1809.04325 [hep-th].

[15] M. Kontsevich and D. Zagier. 'Periods'. *Mathematics Unlimited - 2001 and Beyond*. Ed. by B. Engquist and W. Schmid. Springer, 2001, pp. 771–808.

[16] O. Schnetz. 'Graphical functions and single-valued multiple polylogarithms'. *Communications in Number Theory and Physics* 13.4 (2014), pp. 589–675. arXiv: 1302.6445 [math.NT].

[17] M. Borinsky and O. Schnetz. 'Graphical functions in even dimensions'. *Communications in Number Theory and Physics* 16.3 (2022), pp. 515–614. arXiv: 2105.05015 [hep-th].

[18] D. J. Broadhurst. 'Summation of an infinite series of ladder diagrams'. *Physics Letters B* 307.1 (1993), pp. 132–139.

[19] J. M. Drummond. 'Generalised ladders and single-valued polylogs'. *Journal of High Energy Physics* 2013.2 (2013). arXiv: 1207.3824 [hep-th].

[20] N. I. Ussyukina and A. I. Davydychev. 'Exact results for three- and four-point ladder diagrams with an arbitrary number of rungs'. *Physics Letters B* 305.1 (1993), pp. 136–143.

[21] A. V. Smirnov and F. S. Chukharev. 'FIRE6: Feynman Integral REduction with modular arithmetic'. *Computer Physics Communications* 247 (2020), p. 106877. arXiv: 1901.07808 [hep-th].

[22] N. I. Ussyukina and A. I. Davydychev. 'New results for two-loop off-shell three-point diagrams'. *Physics Letters B* 332.1 (1994), pp. 159–167. arXiv: hep-ph/9402223 [hep-th].

[23] R. Britto, C. Duhr, H. S. Hannesdottir and S. Mizera. 'Cutting-Edge Tools for Cutting Edges'. (2024). arXiv: 2402.19415 [hep-th].

[24] S. Bera. 'MultiHypExp: A Mathematica package for expanding multivariate hypergeometric functions in terms of multiple polylogarithms'. *Computer Physics Communications* 297 (2024), p. 109060. arXiv: 2306.11718 [hep-th].

[25] S. Bera. 'ϵ-expansion of multivariable hypergeometric functions appearing in Feynman integral calculus'. *Nuclear Physics B* 989 (2023), p. 116145. arXiv: 2208.01000 [math-ph].

[26] C. Duhr and F. Dulat. 'PolyLogTools — polylogs for the masses'. *Journal of High Energy Physics* 2019.8 (2019). arXiv: 1904.07279 [hep-th].

[27] M. Besier, D. van Straten and S. Weinzierl. 'Rationalizing roots: an algorithmic approach'. *Communications in Number Theory and Physics* 13 (2019), pp. 253–297. arXiv: 1809.10983 [hep-th].

[28] H. Frellesvig and C. G. Papadopoulos. 'Cuts of Feynman Integrals in Baikov representation'. *Journal of High Energy Physics* 2017.4 (2017). arXiv: 1701.07356 [hep-th].

[29] J. M. Henn. 'Multiloop Integrals in Dimensional Regularization Made Simple'. *Physical Review Letters* 110.25 (2013). arXiv: 1304.1806 [hep-th].